Taiwan — a case study

As we have seen, erosional processes give rise to an exponential decay of the landscape

$$t_{1/2} \approx 40 \text{ Myr}$$

Something must be acting to continually rebuild the landscape, e.g., the collision of India with Eurasia 10 – 20 Myr ago has resulted in the elevation of the Himalayan front (Everest, K-2, Anapurna, ...) and the 5.5 km high Tibetan plateau.

Taiwan offers a type example, on a smaller scale of erosion of an active mountain belt

- steady – state mtn building one of (in a sense to be discussed)
- ↳ fastest erosion rate on ⊕

  ~~⊘⊘⊘⊘⊘⊘~~
  (5 – 6 km /Myr)

one of fastest — S. Alps of NZ are 9 km/Myr

~~For comparison, ... of North America is this is more than ... the world average rate~~

This is 55 times the world average rate $\langle \dot{e} \rangle_\oplus = 0.1$ km/Myr

$$\dot{e}_{Taiwan} = 55 \times \langle e \rangle_\oplus$$

Review geographic and plate tectonic setting — island in China Sea at junction of Ryukyu & Luzon island arcs

Site of an oblique arc-continent collision

To the north the Philippine Sea plate is subducting beneath the Eurasian plate along the Ryukyu arc

To the south the polarity of subduction is reversed — Eurasian plate subducting beneath Philippine Sea plate.

Along Manila trench, this is building a submarine accretionary wedge of the type that is characteristic of all subduction zones, e.g., Barbados
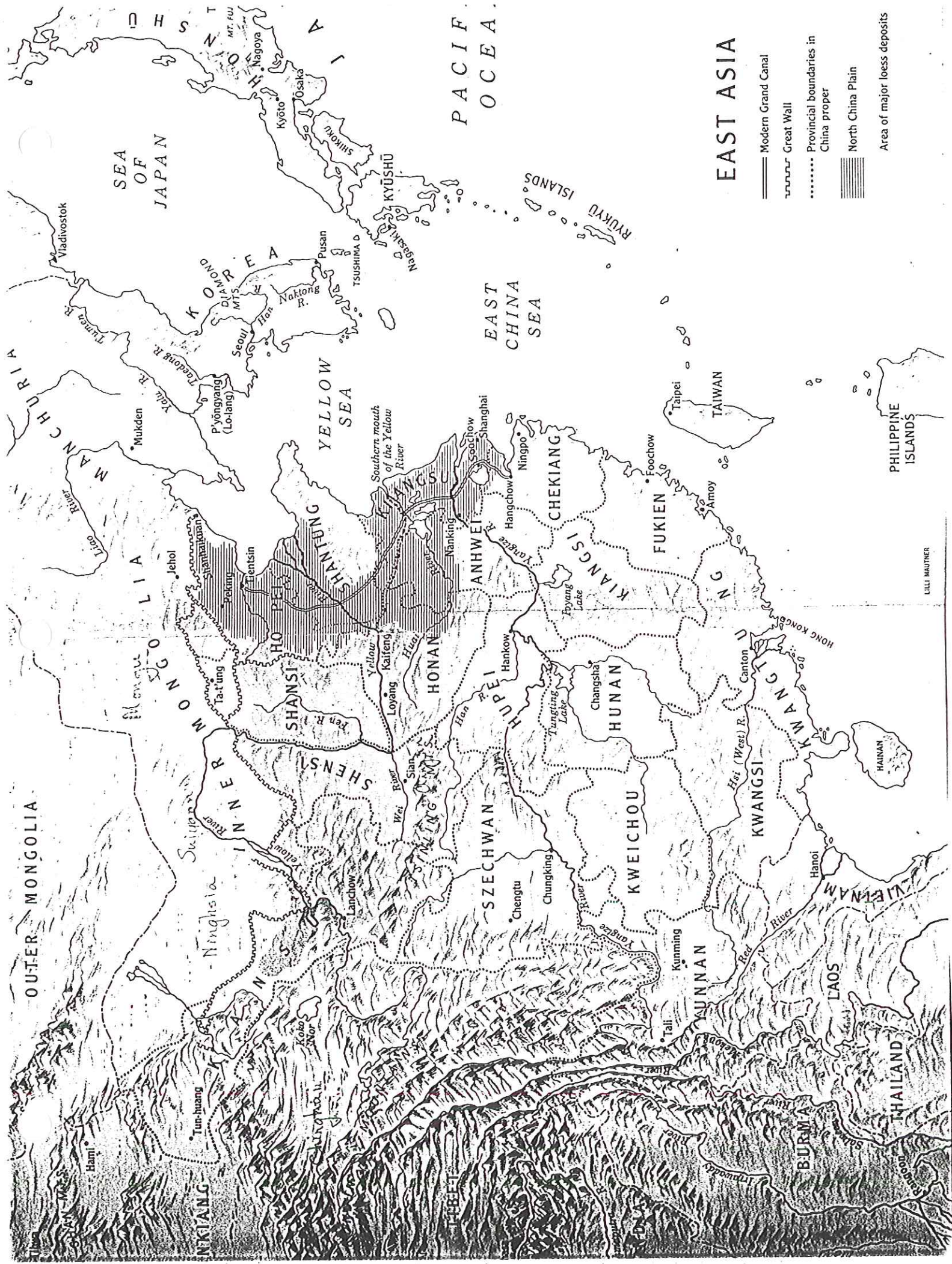
EAST ASIA

─── Modern Grand Canal
┅┅ Great Wall
········· Provincial boundaries in China proper
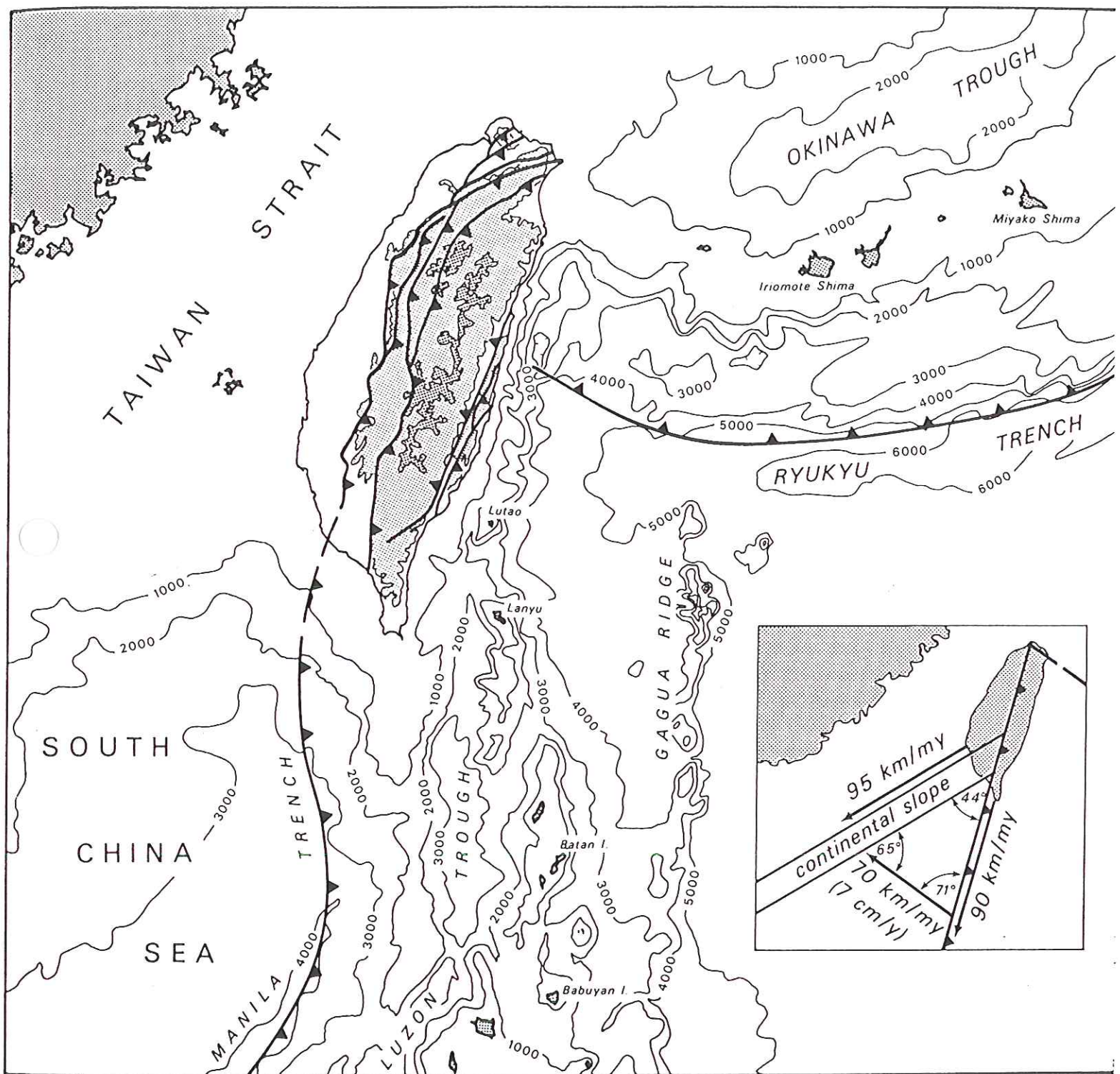▥ North China Plain
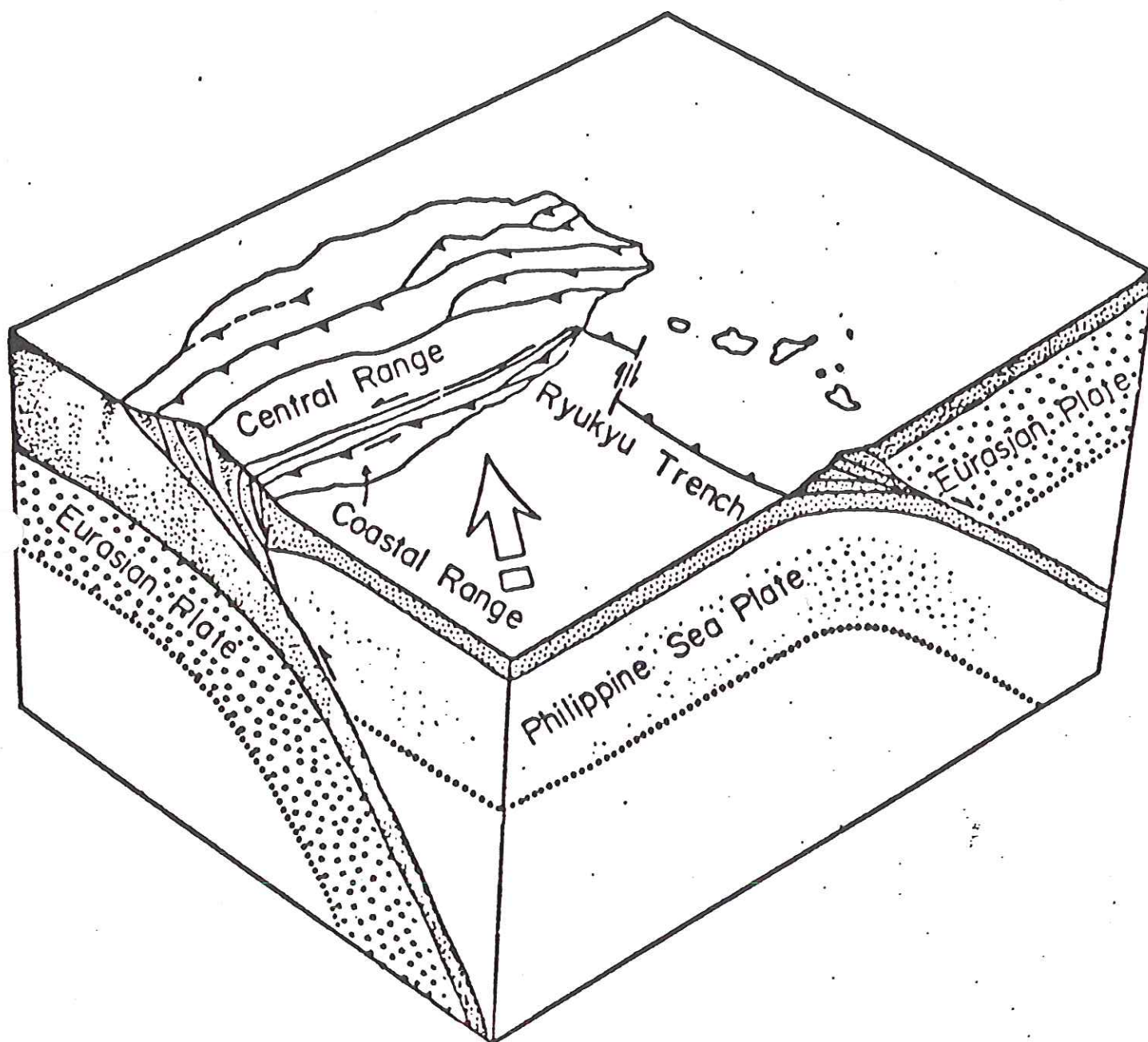▤ Area of major loess deposits

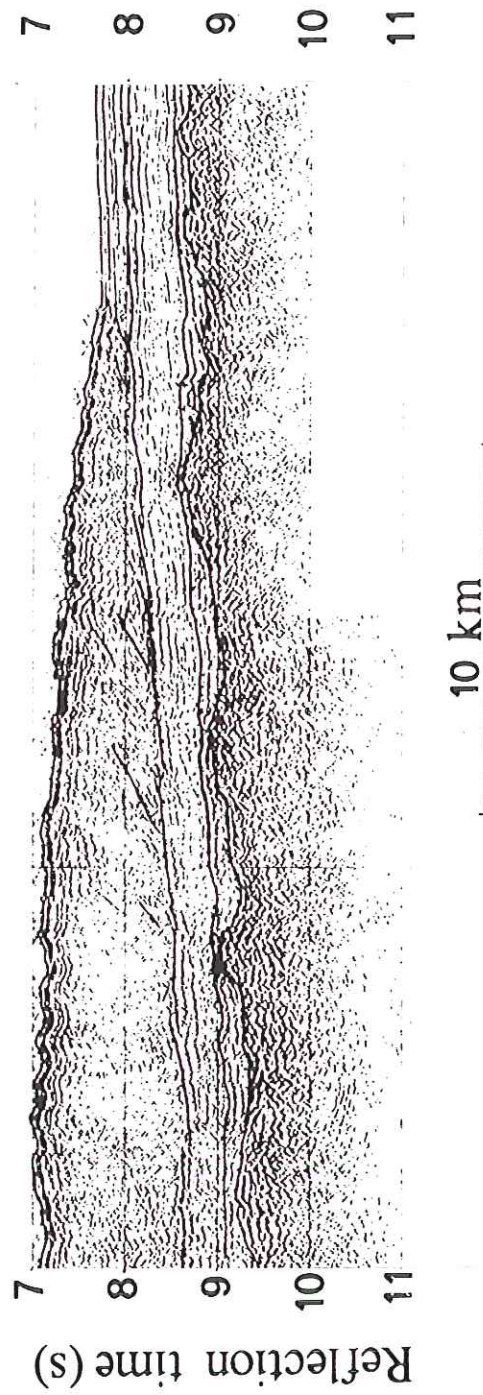LILLI MAUTNER

Fig. 9. Tectonic and bathymetric setting of Taiwan with velocity triangle for arc-continent collision in Taiwan assuming plate motions of *Seno* [1977].

Central Range

Coastal Range

Ryukyu Trench

Eurasian Plate

Eurasian Plate

Philippine Sea Plate

BARBADOS ACCRETIONARY COMPLEX
12–fold stacked and deconvolved
seismic section (Westbrook, et al., 1982)

Reflection time (s)

10 km

E

Chiai

50 km

W

sea level

6½°

Chengkung

4½°

PHILIPPINE SEA PLATE

2.9°

Chiai

6°

ASIAN   PLATE

50 km

Taiwan Topography

0 50 km

300

200

N

Fig. 7

Fig. 6

Fig. 9

100 m

100 m

100

0
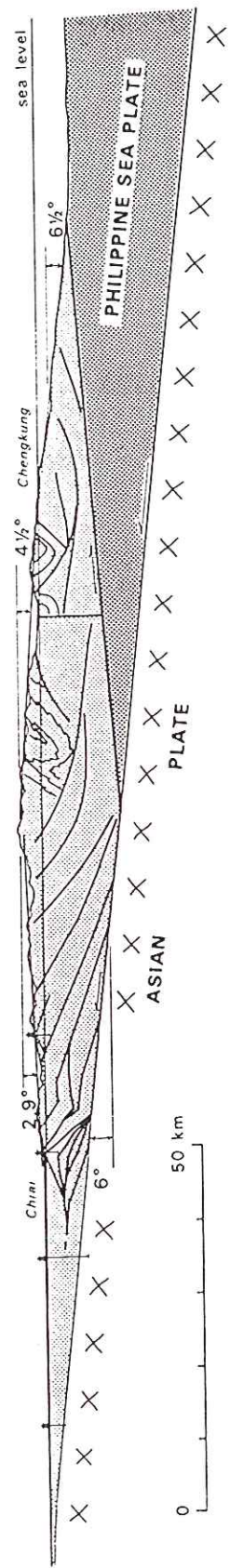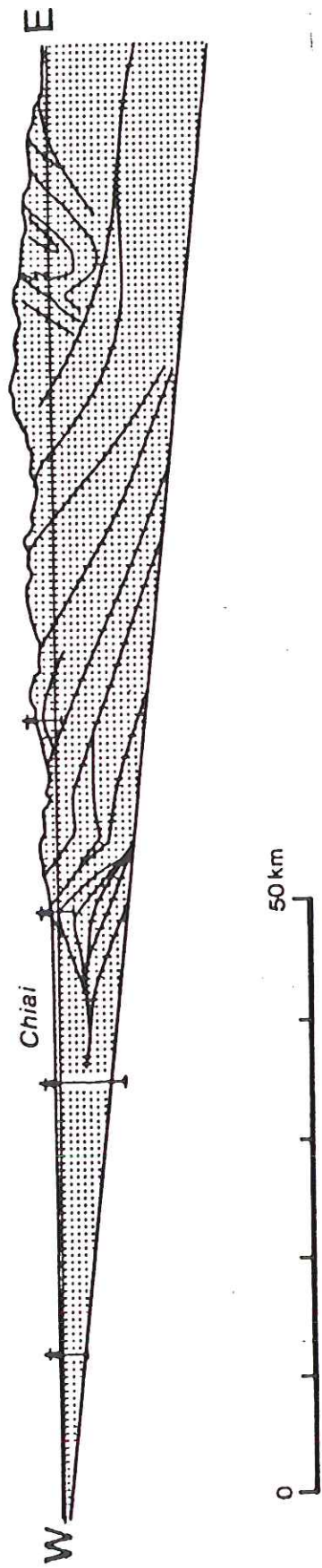
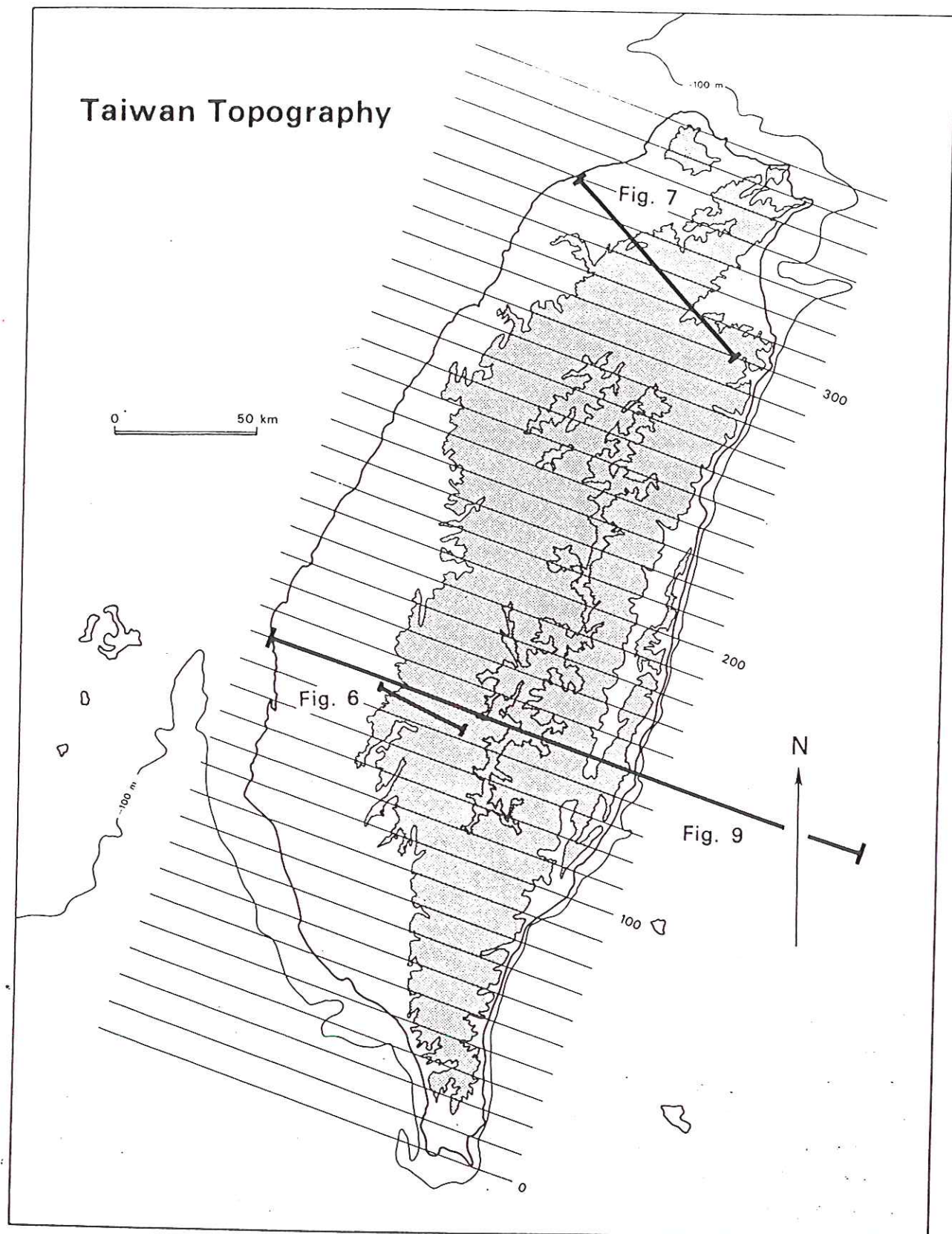Fig. 2. Simplified topography of Central Mountains of Taiwan. Area above 200 m in screened pattern; higher contour is 2000 m. Family of straight lines show locations of topographic profiles in Fig. 4. Profiles are labeled in distance in kilometers N 20°E of southern tip of Taiwan.
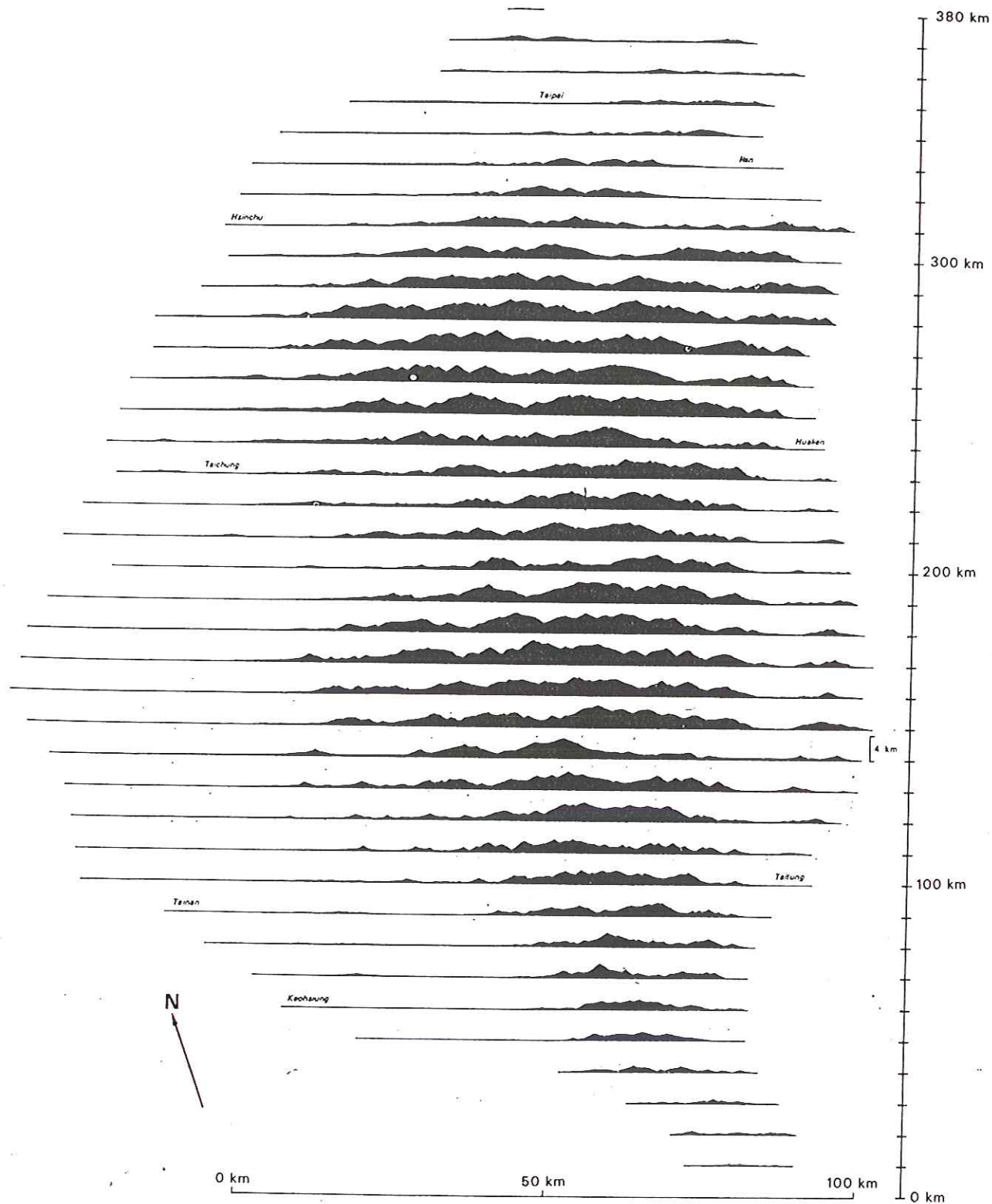
Fig. 4. Topographic profiles of Taiwan along the lines shown in Fig. 2 horizontal scale = vertical scale. Area above sea level shown in black.

Taiwan — the subduction zone is trying to swallow the thick sediments on the China continental margin

Taiwan is an overgrown accretionary wedge that has risen above sea level.

The _mountain_ _building_ due to the collision is _ongoing_ _today_.

The elevated mountain belt is
- 90 km width
- 300 km long

Show John's shaded map and cross-section

The mountains are 2-3 km high and extremely rugged. Very remote, practically uninhabited, except by a few indigenous tribes pushed into the interior when Chiang Kai-Shek and his troops and followers occupied Taiwan upon being expelled from the mainland by Mao.

Almost the entire population lives in the ~~XXXX~~ western coastal plain

The erosion rate in Taiwan can be measured in a number of independent ways. The good agreement between these diverse methods gives us great confidence in the result.

- stream gaging — measure sediment load at mouths of the ~~major~~ major rivers.

$$\boxed{\text{Total sediment load } 380 \cdot 10^6 \frac{\text{tons}}{\text{yr}}}$$

Erosion rate:

$$\frac{380 \cdot 10^6 \text{ tons/yr} \times 10^6 \text{ yr/Myr}}{2500 \cdot 10^6 \text{ tons/km}^3 \times 90 \times 300 \text{ km}^2}$$

density of sedimentary rock ↗

elevated area

$$= 5.6 \text{ km/Myr}$$

↳ this is a direct measurement of $\dot{e}$ Taiwan

over past 50–100 yrs

~~Already state width of mountain belt~~

~~the nearly constant 90 km width~~

The number $350 \cdot 10^6 \frac{tons}{year}$ is huge.

In comparison, from all of North America

$$1020 \cdot 10^6 \frac{tons}{year} \quad (North\ America)$$

Taiwan $\approx$ 40% North America!

All the factors that increase the erosion rate conspire in Taiwan:

- very high precipitation rate
- tropical climate — lush vegetation (bamboo, etc.)
- sedimentary rock — mostly shale — carbonaceous cement — easily weathered
- rock deformed by collision & mountain building — faults, etc. — more easily eroded
- extremely rugged relief.

Could also say: US total = $400 \cdot 10^6 \frac{tons}{yr}$
conterminous

Taiwan $\approx$ conterminous US

**TABLE 5.2** Suspended Sediment Carried by Rivers to the Ocean (in Metric Tons)

Continent	Drainage Area Contributing Sediment to Ocean (10^6 km^2)	Sediment Discharge (10^6 tons/yr)	Sediment Yield (tons/km^2/yr)	Mean Continental Elevation (km)
North America	15.4	1020	66	0.72
Central America[a]	2.1	442	210	—
South America	17.9	1788	97	0.59
Europe	4.61	230	50	0.34
Eurasian Arctic	11.17	84	8	~0.2
Asia	16.88	6349	380	0.96
Africa	15.34	530	35	0.75
Australia	2.2	62	28	0.34
Pacific & Indian Ocean Islands[b]	3.0	9000[c]	3000[c]	~1.0
World total	88.6	20,000[d]	226[d]	

[a] Includes México.

[b] Japan, Indonesia, Taiwan, Phillipines, New Guinea, and New Zealand (Oceania).

[c] From Milliman and Syvitski (1992).

[d] From Milliman and Syvitski (1992). Data reflect greater sediment discharge from South America, the Alps-Caucusus Mountains, and northwest Africa, in addition to Oceania.

Sources: After Milliman and Meade (1983) and Milliman and Syvitski (1992), elevations from Fairbridge (1968).

• Method 2 (somewhat indirect) — steady-state width of mountain belt

nearly constant 90 km width suggests accretionary flux in = erosive flux out

analogy — bulldozer wedge in a rainstorm

accretionary
flux
in
at toe

$\dot{e}$

width W

subduction
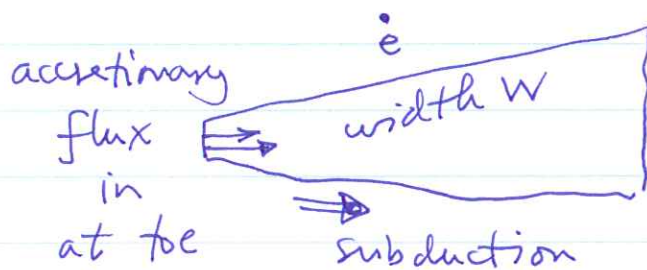
hV

$h =$ thickness of deformed
wedge at toe — seismic
data — 7 km

$V =$ plate ~~tecto~~ convergence velocity
known from plate tectonics
70 km/Myr

steady-state:
$$hV = \dot{e}W$$

$$\dot{e} = \frac{hV}{W} = \frac{7 \text{ km} \times 70 \text{ km/Myr}}{90 \text{ km}}$$

$$= 5.5 \text{ km/Myr} \text{ — indirect but}$$
in excellent
agreement

A 200-km-long segment of the **Taiwan fold-and-thrust belt** between 23° N and 25° N is in steady-state.

- $V = 70$ km/Ma: local plate convergence rate
- $h = 7$ km: deep drilling and seismic profiling
- $\dot{e} = 5.5$ km/Ma: streamload data, radiocarbon and fission-track dating
- $W = 90$ km: width of the steady-state region
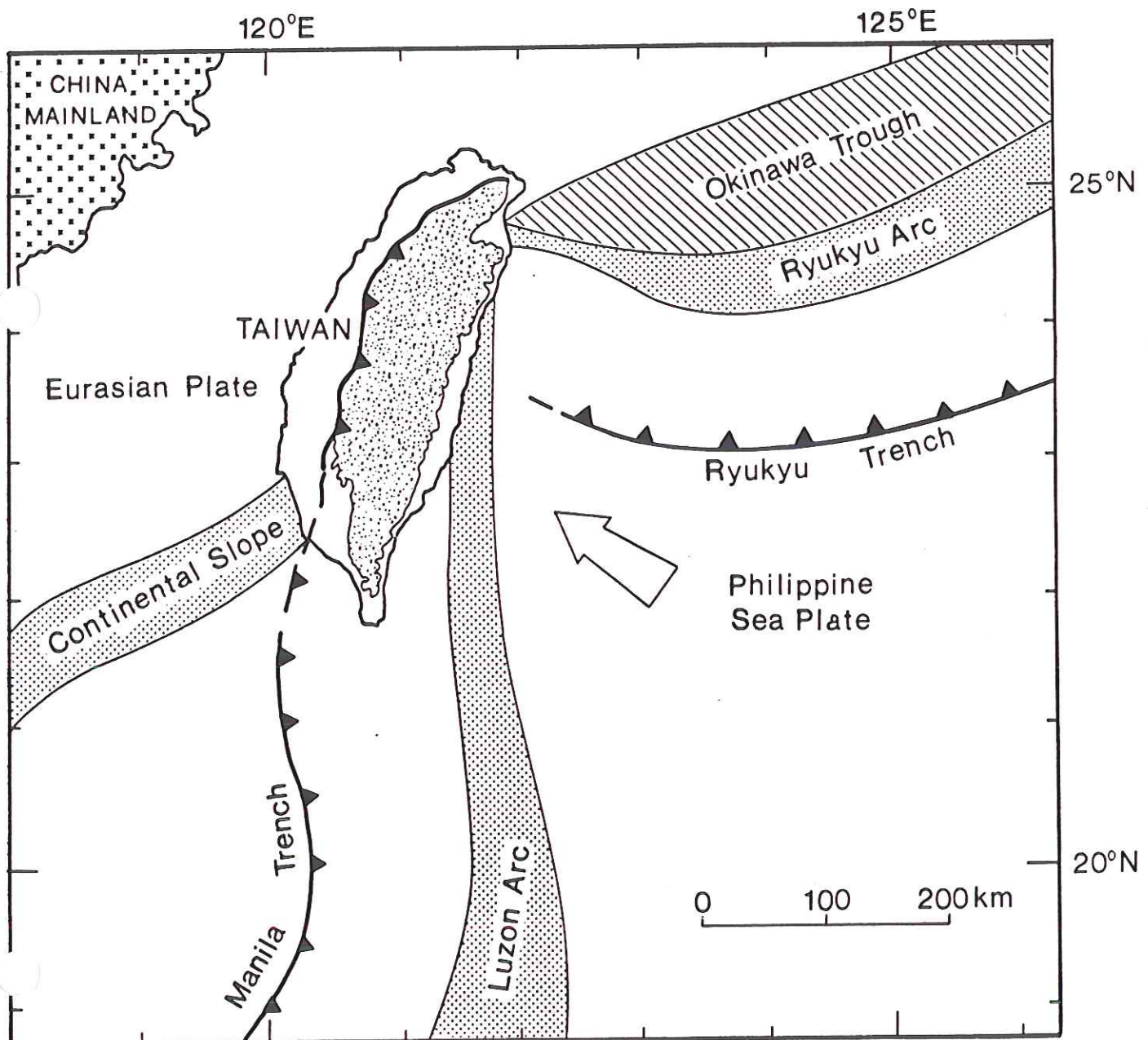
- accretionary influx: hV = thickness of entering section × plate convergence velocity

- erosive efflux: $\dot{e}W$ = erosion rate × width of fold-and-thrust belt
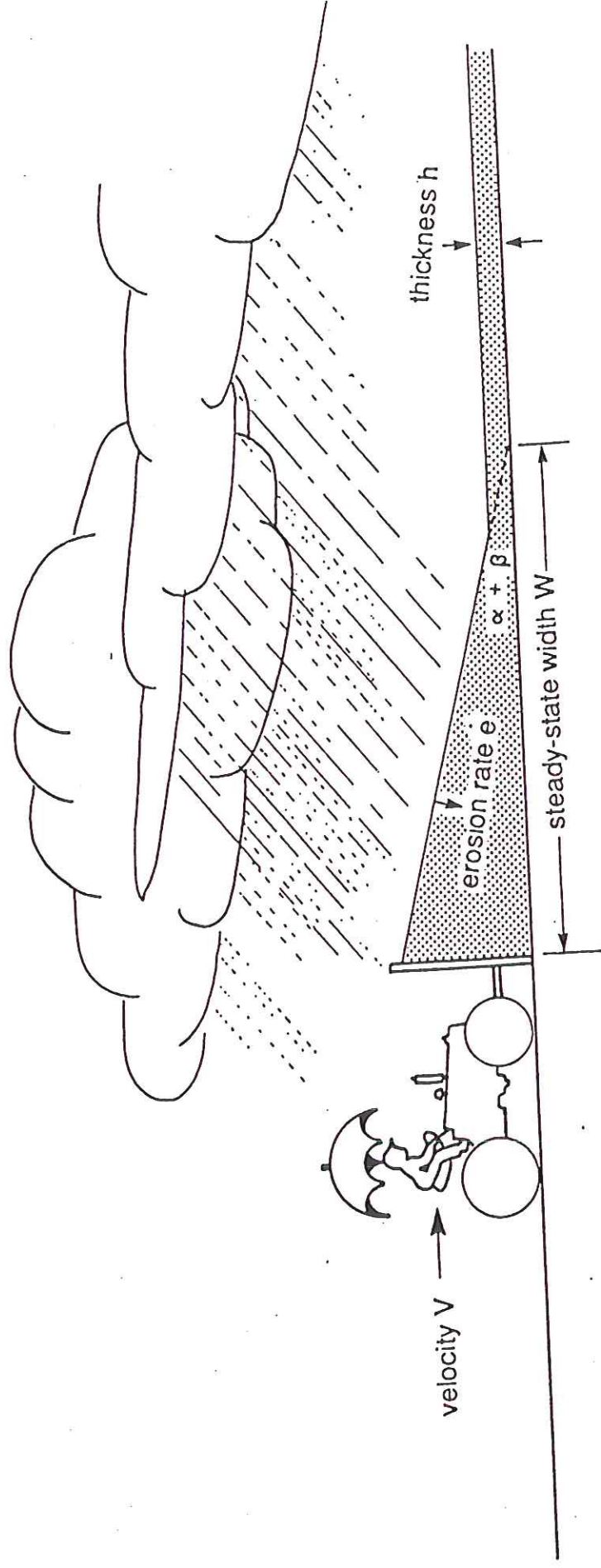
Fig. 7. Simplified structural cross section of northern Taiwan (after Suppe. 1980a). Location of cross section shown in Fig. 2.
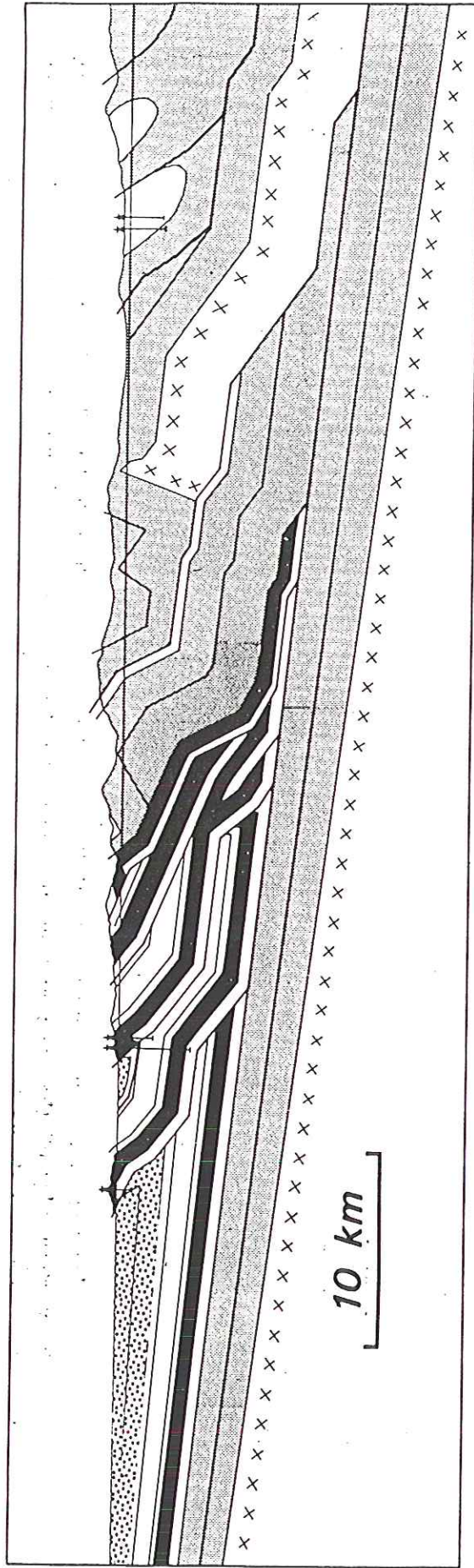
So, just like the bulldozer wedge in the rainstorm, the $\underline{shape}$ of the mountains is constant in time

New rocks are being $\underline{uplifted}$ by mountain building processes to replace the eroded rocks — there is $\underline{no}$ $\underline{decay}$ of the $\underline{landscape}$.

$\dot{e}$ is also a measure of the $\underline{uplift}$ $\underline{rate}$

There are two ways the $\underline{uplift}$ $\underline{rate}$ can be measured:

As uplift occurs, streams cut ever deeper into their floodplains leading to the formation of $\underline{terraces}$
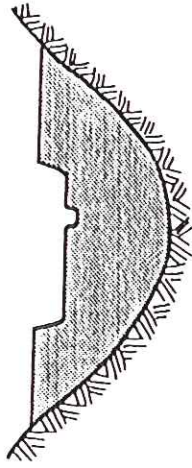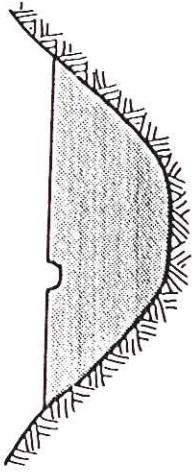
- ^{14}C dating of uplifted terraces

Just measure terrace heights above sea level and ^{14}C date charcoal, etc. Can also ^{14}C date uplifted corals found in a few localities along coast

result: $\dot{e} \cong 5$ km/Myr — again

Erosion of valley → Deposition of alluvial fill → Erosion of alluvial fill

Flood plain

A

Terrace

Flood plain

B
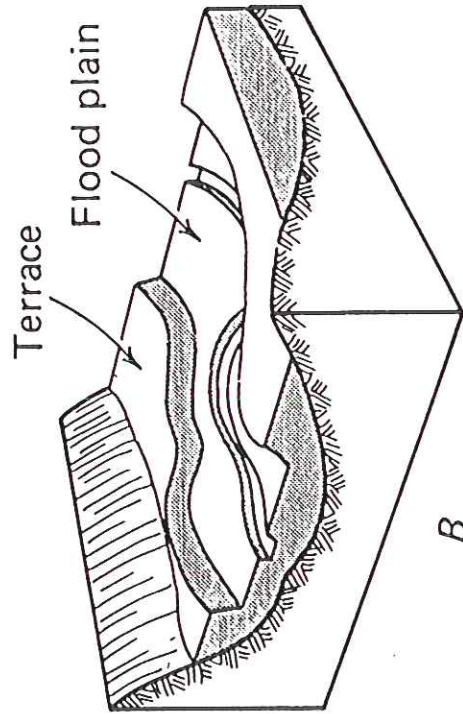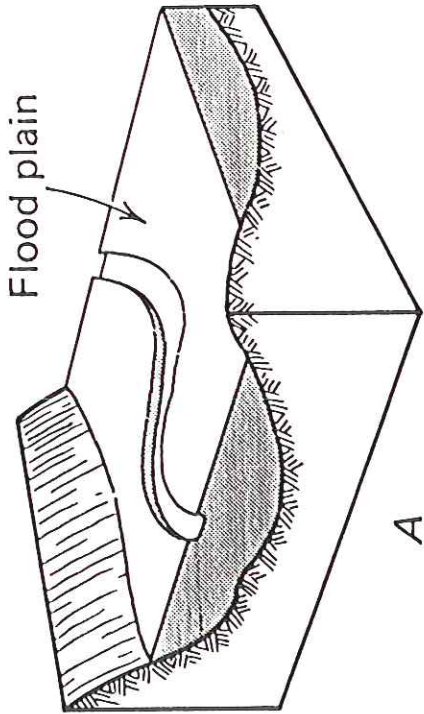
- Yet another measure — fission track and $^{40}Ar - ^{39}Ar$ dating of rocks that have been uplifted from deep, now in the high mountains

Describe our thermal ⬤ model — accounts for frictional heating on the decollement fault — fits heat flow which is high — particularly in the eastern high mountains

$$90 \frac{mW}{m^2} \quad to \quad 240 \frac{mW}{m^2}$$

Corresponding thermal gradients

$$27°C/km \quad to \quad 70°C/km$$

extremely high gradient — many hot springs in eastern Taiwan

Knowing P and T within the mountain belt, can infer P-T-t trajectories

another steady state box model!

The residence time of an average rock before it is uplifted and eroded is 2-3 Myr.

The temperature time histories can
be measured, e.g. biotite has
an ~~Ar~~.Ar <u>blocking</u> temperature of 300°C.

When heated above that, Ar diffuse out
so rapidly that none is retained
Thus $^{40}Ar - ^{39}Ar$ age is age when rock
cooled below 300°C

Fission tracks — damage in xtal
lattice due to spontaneous fission — are
<u>annealed</u> at ~~even~~ even lower temperatures.

The model does an excellent job
of fitting T—t data, e.g. for
a single rock from Chipan

Work of Chinghua Lo & Tullis Onstott

Note this provides another independent
estimate of erosion rate

The apatite xtals in the rock at
Chipan ~~cooled through~~ dropped
in temperature by 115° while
being uplifted along a 50°C/km
geotherm in 0.4 Myr

$$\frac{115°C}{50°C/km \times 0.4 \, Myr} = 5.5 \, km/Myr$$

Smoothed surface heat flow (mW/m²)

Chingtsaohu
$T_0' = 27°C/km$

depth (km)

temperature (°C)

100 km
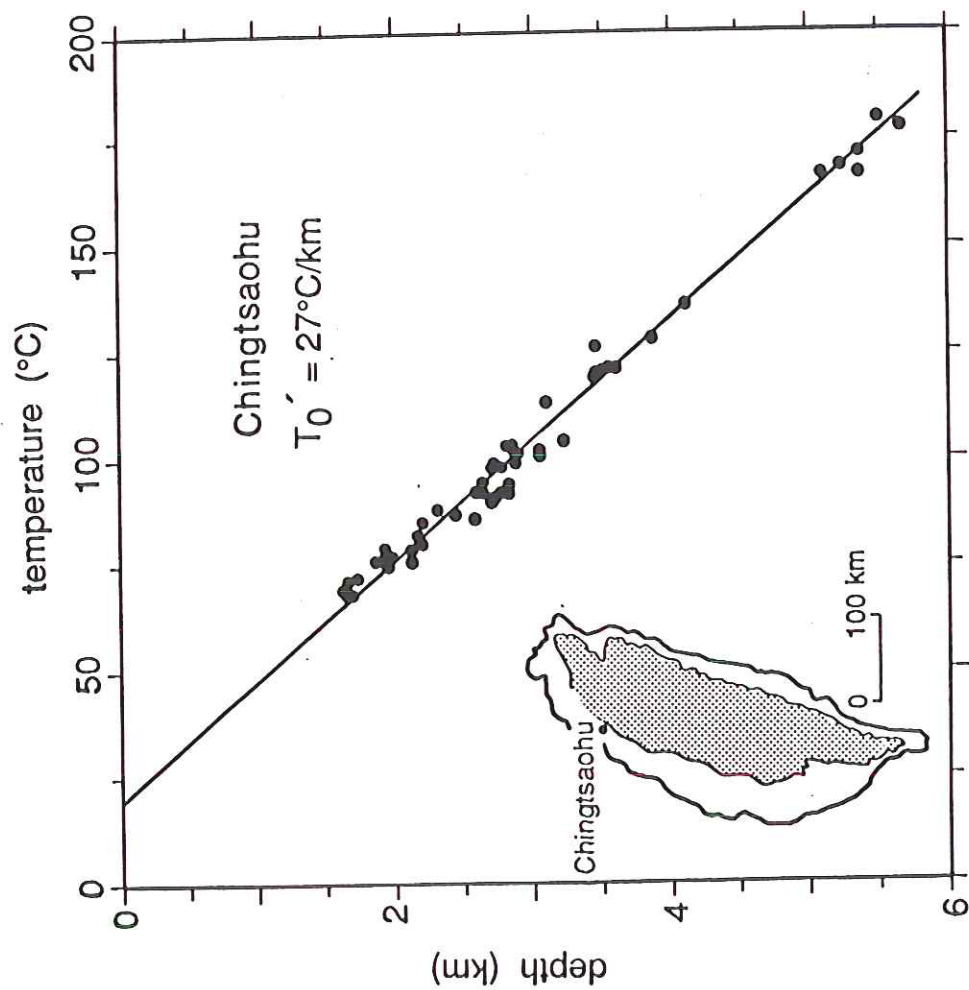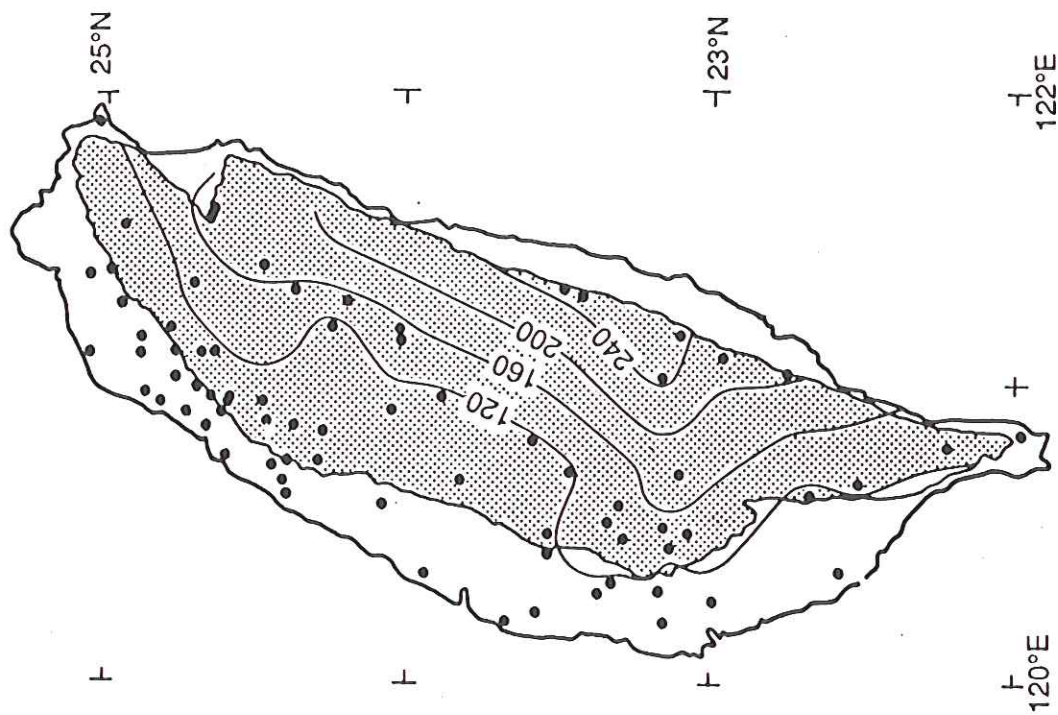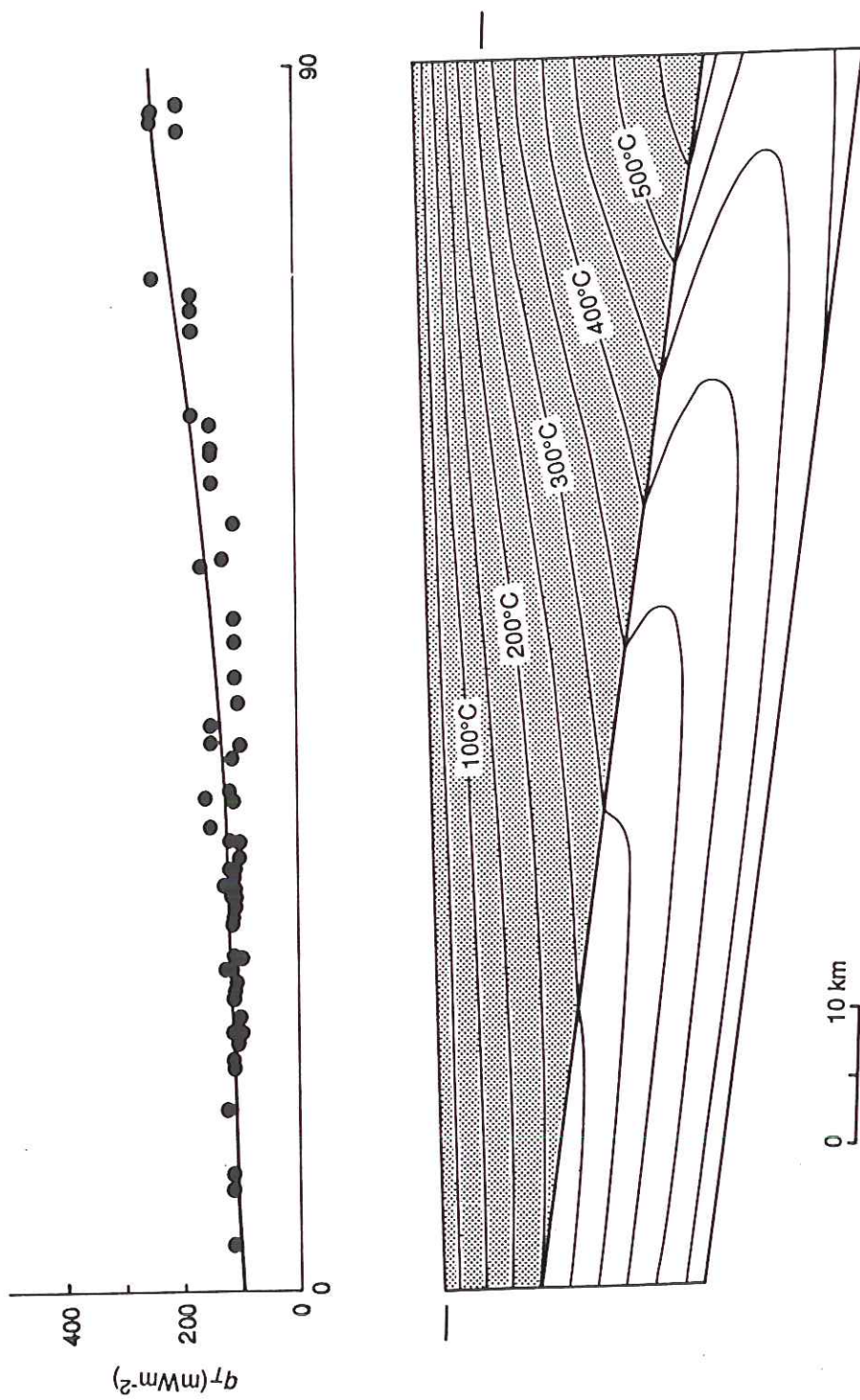
The thermal model also predicts the theoretical pressure-temperature-time or **P-T-t trajectories** of rocks that outcrop at the surface. Any information about the P-T-t paths that is preserved in the rocks provides an alternate source of data.

temperature

solid pressure $P = -\frac{1}{2}(\sigma_1 + \sigma_3)$

particle trajectories

90 km

7 km
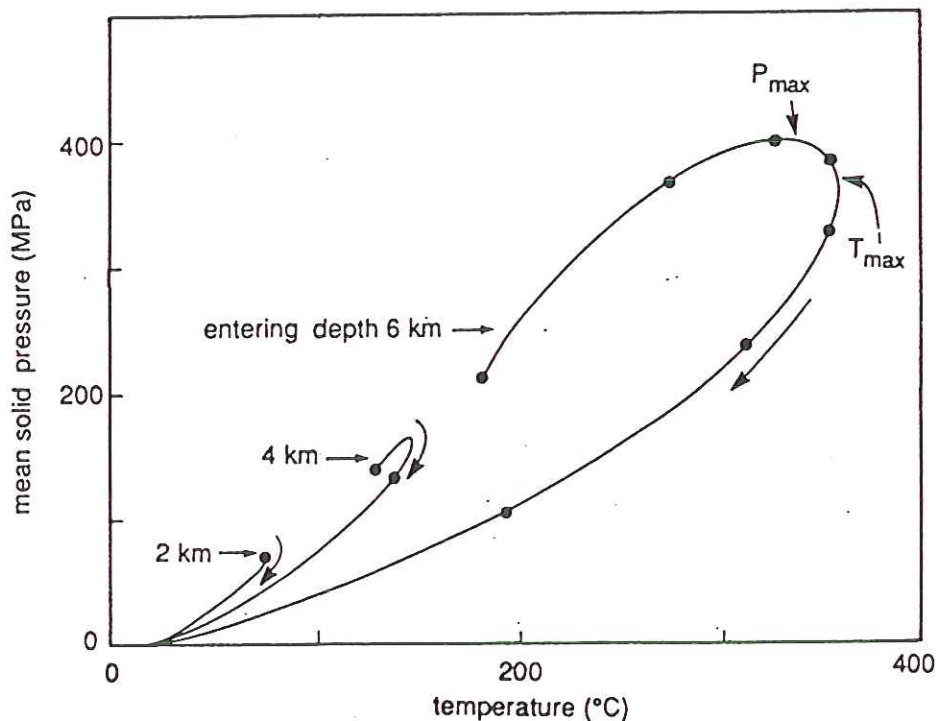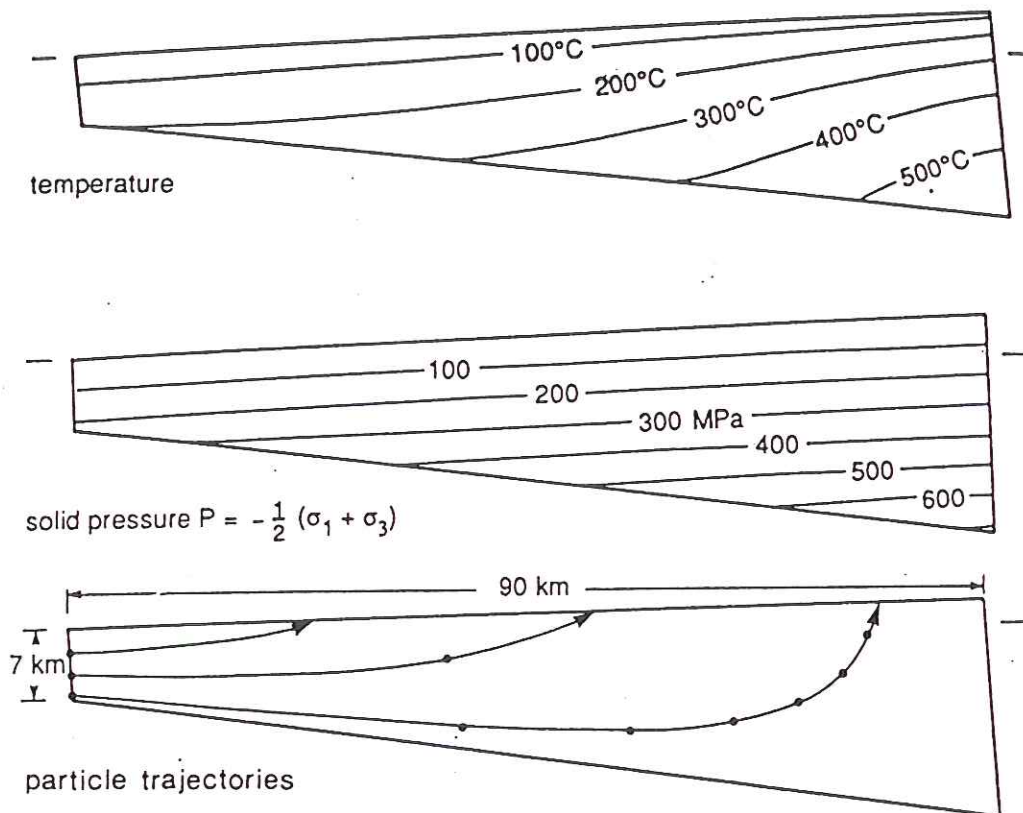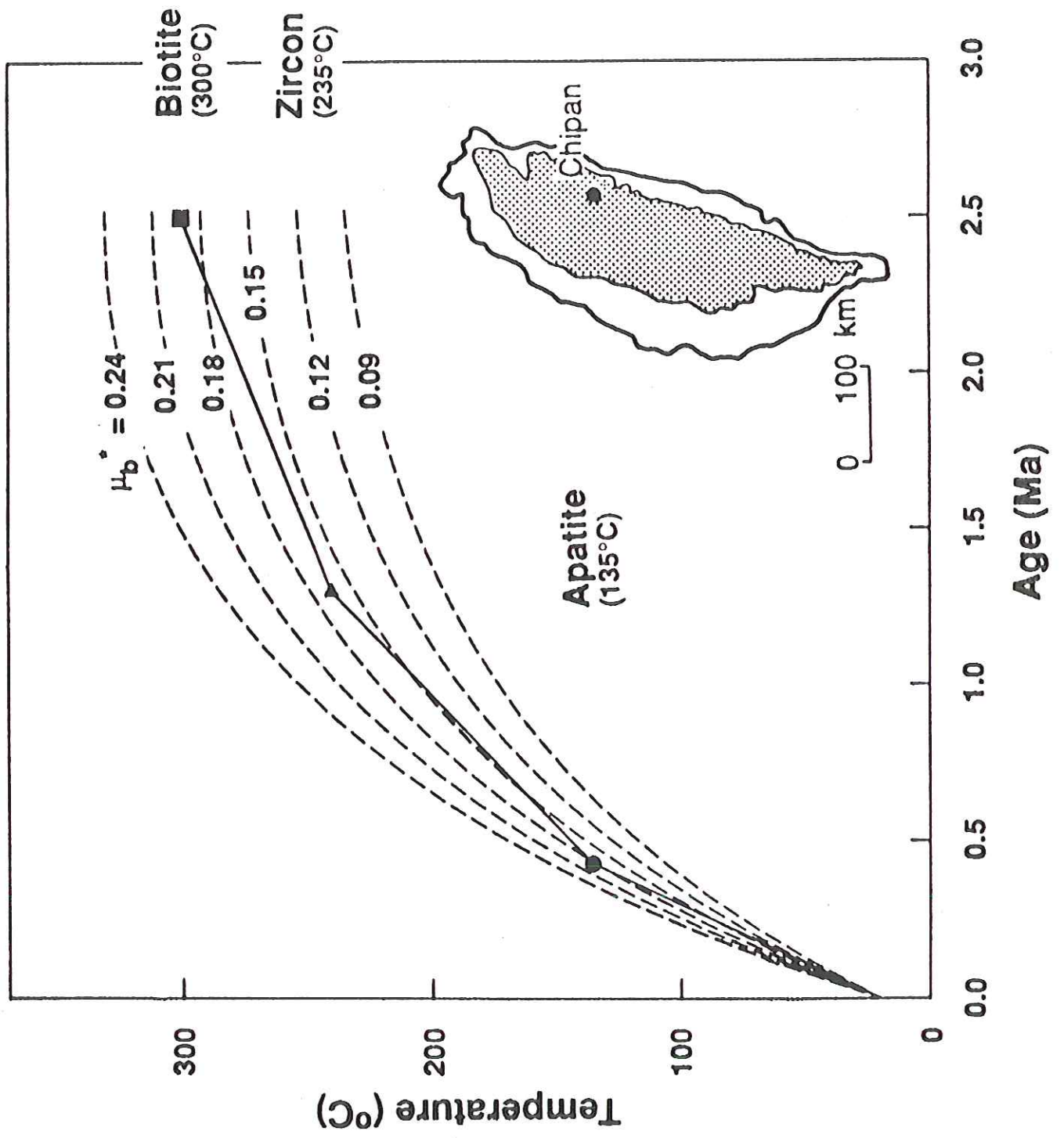
Becky Dorsey's work provides yet another independent determination.

Looked at sediments shed from the mountains.

Used fossils to date these and detailed
/ nanofossil ages
petrological analysis to deduce the metamorphic grade of the source rocks

Clear unroofing trend youngest sediments unmetamorphised, 4 Myr old sediments most metamorphosed.

Conclusion: biotite grade rocks uplifted from 12 - 15 km depth in 3 Myr ⟹

$$\dot{e} = 3.9 - 4.8 \ km/Myr$$

TABLE 3.—*Calculation of uplift rate*

TIMING of collision-related metamorphism, based on plate kinematic and stratigraphic studies (Suppe 1981; Chi et al. 1981; Buchovecky 1986), about 4.5 Ma.

CONDITIONS of metamorphism, based on petrology and geochemistry of metamorphic rocks in the Central Range (Ernst 1983),

$$Lm1: T = 325° \pm 75°C \qquad P = 3 \text{ kbar (chlorite grade)}$$
$$Lm2: T = 425° \pm 75°C \qquad P = 4 \text{ kbar (biotite grade)}.$$

DEPTH of metamorphism: Modern geothermal gradient in western Taiwan (Suppe and Witke 1977) = 30°C/km. Assuming lithostatic gradient of about 3 km/kbar, depth of Lm2 metamorphism = 12–15 km.

TIMING of surface erosion of biotite-grade (Lm2) metamorphic rocks based on ternary Ls-Lm1-Lm2 diagram (this paper), about 1.4 Ma (= midpoint of lower NN19).

RATE of uplift: Biotite-grade metamorphic rocks uplifted from 12–15 km depth to the surface between about 4.5 and 1.4 m.y. (= 3.1 m.y.): Uplift rate = 3.9 to 4.8 km/m.y.

FIG. 6.—Ternary diagram of lithic fragments defined in this paper: sedimentary (Ls); low-grade metamorphic (Lm1); and medium-grade metamorphic (Lm2). A) Distribution of sandstones within a well-defined compositional field. Note that the oldest samples plot near the Ls corner, and younger samples become progressively enriched first in Lm1 and later in Lm2. B) Same diagram plotting means and standard deviations of each age group. Note the strong age dependence of the compositional trend; this reflects unroofing of the (meta)sedimentary complex through time and erosion into progressively deeper (higher-grade) levels in the collision belt.

In summary we think we understand the steady-state mtn building in Taiwan __very well__.

~~Five~~ independent measurements of erosion rate $\dot{e}$:

- streamload data — direct
- dating of uplifted terraces & corals ^{14}C
- fission track and $^{40}Ar - ^{39}Ar$ dating of metasedimentary rocks
- accretionary influx ÷ width
  $$\dot{e} = hv/w \quad \text{in steady state}$$
- metamorphic unroofing rate (B. Dorsey)

Note these are measurements of $\dot{e}$ averaged over different intervals of time

sixth method sept 2002
direct bedrock incision measurements

- streamload — last 100 years
- ^{14}C — last 5000 - 10,000 years
- Ar dating — last 2-3 Myr
- steady-state — ditto
- Becky Dorsey — unroofing rate ditto

Good agreement indicates that modern streamloads are indicative of pre-man erosion rates — no influence of man in Taiwan Reason: they all live in the coastal plain; all erosion in mountains

Climate-Driven Bedrock Incision in an Active Mountain Belt

Karen Hartshorn,[1] Niels Hovius,[1] W. Brian Dade,[2]
Rudy L. Slingerland[3]

Fig. 1. (A) Location of study site within Taiwan. (B) Photograph of site from upstream. Black circles represent the location of transect drilled and measured on quartzite, and black diamonds represent the location of the schist transect. White arrow shows the high-water mark, approximately equivalent to the high point of Supertyphoon Bilis. The metal cage and overhead cables indicate the location of discharge and the suspended sediment gauging station. (C) Cross section of the channel along the quartzite outcrop with survey points, showing characteristic parabolic shape with steep side walls. The wavy line represents the low-water mark.

Spatially averaged erosion of both rock types between December 2000 and December 2001 approached values of 2 to 6 mm year^{-1} and occurred near the base of the channel. These incision rates are in good agreement with independent estimates of long-term exhumation at 3 to 6 mm year^{-1} mentioned above.

Our data indicate that the lowering of the LiWu valley is driven by relatively frequent flows of low to moderate intensity (21) and that rare large floods are more important in widening the bedrock channel than they are in driving down the base level. However, such floods help transmit the effect of accumulated thalweg lowering to adjacent hillslopes.

Are modern streamload erosion
rate measurements geologically
representative?

Many possible human effects:

- agriculture — soil erosion from
  plowed fields
- deforestation — conversion to
  cropland

- overgrazing
- effect of forest fires
- dams — trap sediments,
  e.g., Lake Mead
- groundwater "mining" —
  decreases streamflow
- channelization & other
  flood control measures

Assessing the impact of man is
not easy.

In Taiwan we could compare
modern estimates of $\dot{e}$ with
long-term averages over the past
2-3 Myr.

Case Study 2 — Huanghe (Yellow) River
       in China

Here, in contrast, the influence of
man has been profound.

Recall, the Huanghe drains the
extensive loess deposits of China

Has second largest sediment load
in the world — after the Amazon

$$\boxed{1100 \cdot 10^6 \text{ tons of sediment / year}}$$

Practically all suspended load — Yellow River

This huge load belies the small size
of the drainage area:

$$0.8 \cdot 10^6 \text{ km}^2 \approx \text{ size of Yukon river basin in Alaska}$$

but sediment load $\approx 20 \times$ Yukon!

Question — what if anything has been the
effect of man on this high erosion rate?

TABLE 5.1 Major Rivers that Flow to the Sea, Listed in Order of Discharge

| River | Location | Annual Discharge | | | Dissolved/ Suspended Ratio | Drainage Area (10^6 km^2) |
		Water (km^3/yr)	Dissolved Solids (Tg/yr)	Suspended Solids (Tg/yr)		
1. Amazon	S. America	6300	275	1200	0.23	6.15
2. Zaire (Congo)	Africa	1250	41	43	0.95	3.82
3. Orinoco	S. America	1100	32	150	0.21	0.99
4. Yangtze (Chiang)	Asia (China)	900	247	478	0.53	1.94
5. Brahmaputra	Asia	603	61	540	0.11	0.58
6. Mississippi	N. America	580	125	210 (400)	0.60	3.27
7. Yenisei	Asia (Russia)	560	68	13	5.2	2.58
8. Lena	Asia (Russia)	525	49	18	2.7	2.49
9. Mekong	Asia (Vietnam)	470	57	160	0.36	0.79
10. Ganges	Asia	450	75	520	0.14	0.975
11. St. Lawrence	N. America	447	45	4	11.3	1.03
12. Parana	S. America	429	16	79	0.20	2.6
13. Irrawaddy	Asia (Burma)	428	92	265	0.35	0.43
15. Mackenzie	N. America	306	64	42	1.5	1.81
17. Columbia	N. America	251	35	10 (15)	3.5	0.67
20. Indus	Asia (India)	238	79	59 (250)	1.3	0.975
Red (Hungho)	Asia (Vietnam)	123	?	130	?	0.12
Huanghe (Yellow)	Asia (China)	59	22	1100	0.02	0.77

Note: Tributaries are excluded. Tg = 10^6 tons = 10^{12} g.

Sources: Water and suspended solids from Milliman and Meade (1983) and Milliman and Syvitski (1992). Dissolved solids calculated from Table 5.7 and Pinet and Souriau (1988) (for the Irrawaddy). Suspended load values in parentheses indicate pre-dam values.

(c)

Haerbing

Peking

Hwang
Ho

Wuhan

Canton

Gobi
Desert

Wulumuqui

Ordos

Tengri

Chengdu

Altai

Tien Shan

Tarim
Basin

Aerh-chin shan

Kun Lun Shan

Yangtze R.

Tibetan Plateau

Lhasa

Pamirs
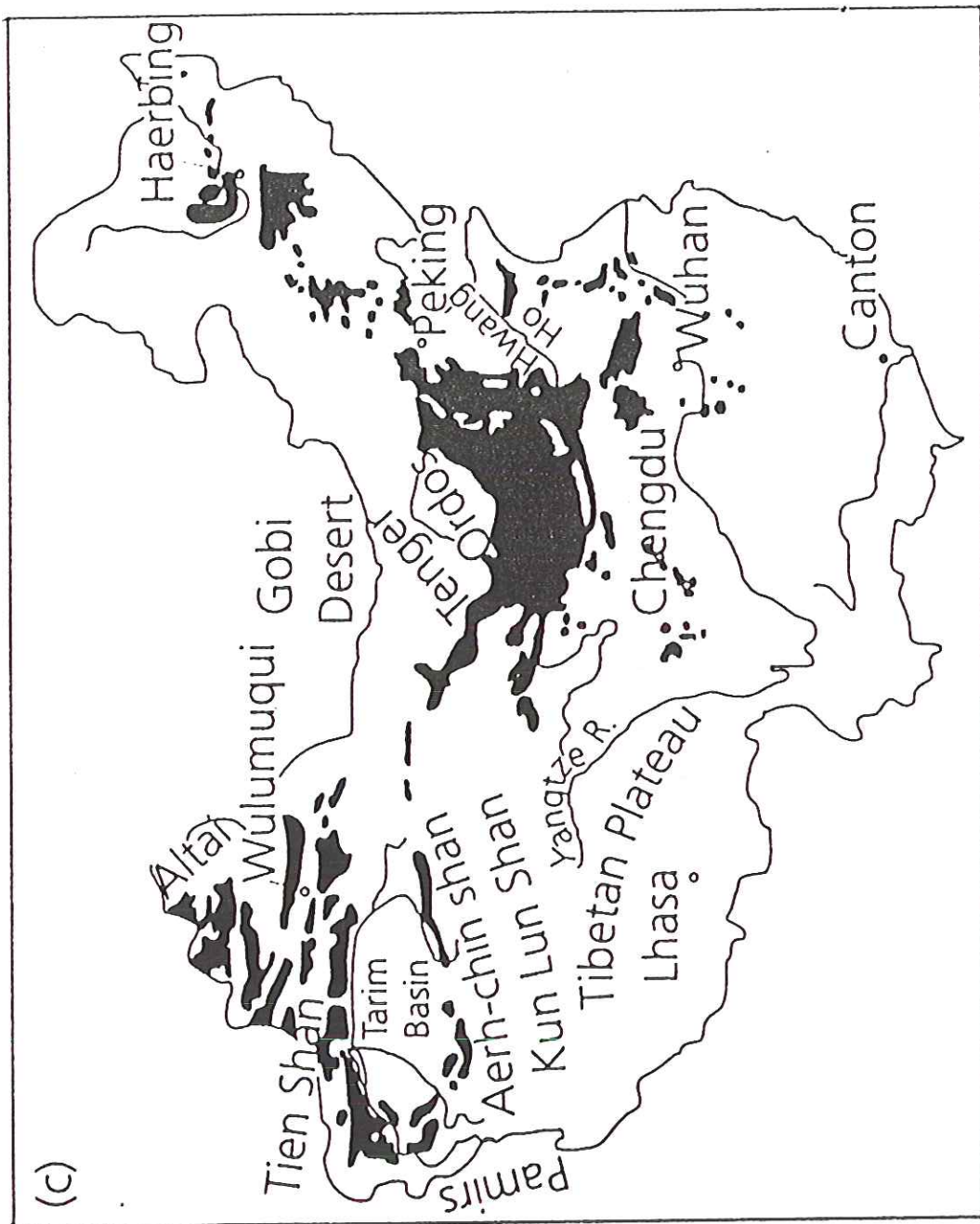
List possible effects of human population growth on measured erosion rates — as seen, e.g., in modern streamload data

- agriculture — soil erosion of plowed fields
- dams — trap sediments (Lake Mead homework problem)
- groundwater "mining" — ~~decreases~~ decreases stream flow
- ~~effect of forest fires~~
- deforestation — conversion to cropland — increased runoff — homework
- channelization — flood control
- overgrazing
- effect of forest fires

Many possible human effects — definitely an important issue.

Are modern erosion estimates geologically representative — we have seen that this is ~~not~~ the case in Taiwan.

Not an easy question to answer — in Taiwan required comparison of different timescale measurements.

Homework problem — effect of man in U.S.

1620

1920

Each dot represents
25 000 acres
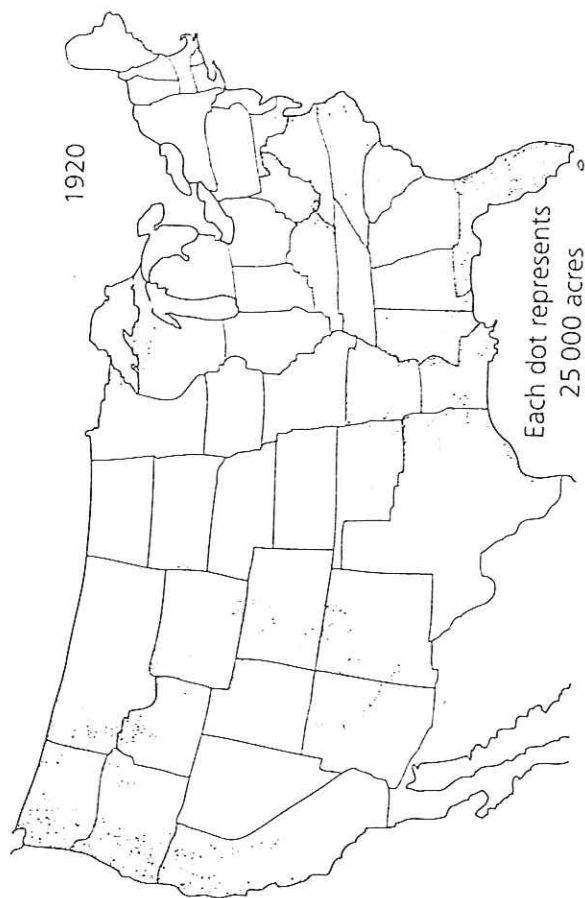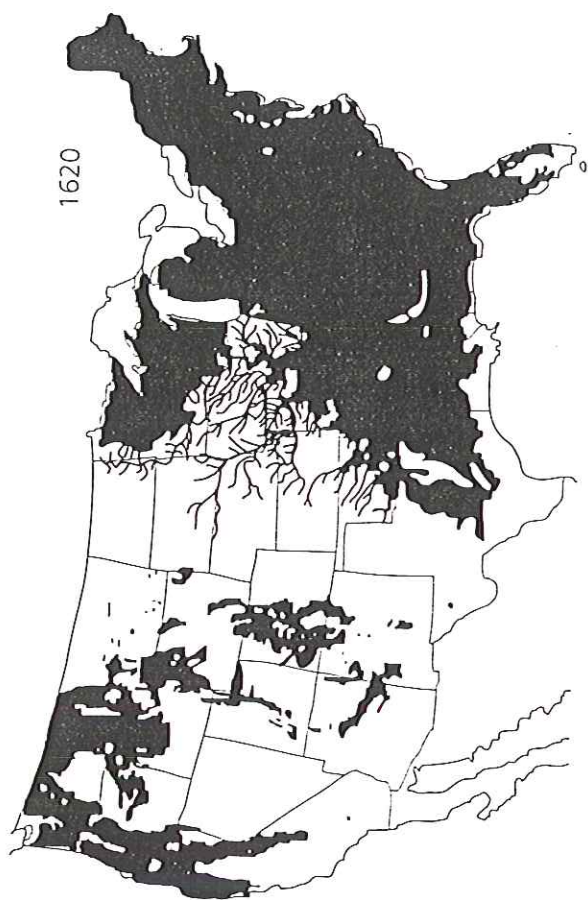
Fig. 3.34 Loss of forest due to
human colonization of North
America between 1620 and 1920.
After Goudie (1993) [47].

What is the present-day erosion rate?

$$\frac{1.1 \cdot 10^9 \frac{ton}{yr} \cdot 10^6 \frac{yr}{Myr}}{0.8 \cdot 10^6 \, km^2 \cdot 2500 \cdot 10^6 \frac{ton}{km^3}} = 0.6 \frac{km}{Myr}$$

$$= \frac{1}{10} \text{ Taiwan}$$

But... is this representative
of the pre-man geological average?

Study 1987 by Milliman & al

China has a long recorded history —
we know a lot about last 2300
years. We know, for example,
that the river has changed courss
during this interval (see map)

Sometimes mouth in Gulf of Bohai
(e.g., now), sometimes in Yellow
Sea (e.g., 1495 - 1855). The various
dynasties have struggled with _ over
1000 years ago built Grand Canal to
re-channel H_2O supply from one mouth
to the other.

ambitious
plans to
upgrade
Grand Canal
even
now.

Accounting for the documented changes in
land usage (Mongol invasion, etc.)
Milliman & al find a total of
$$\boxed{2290 \cdot 10^9 \text{ tons in past 2300 yr}}$$
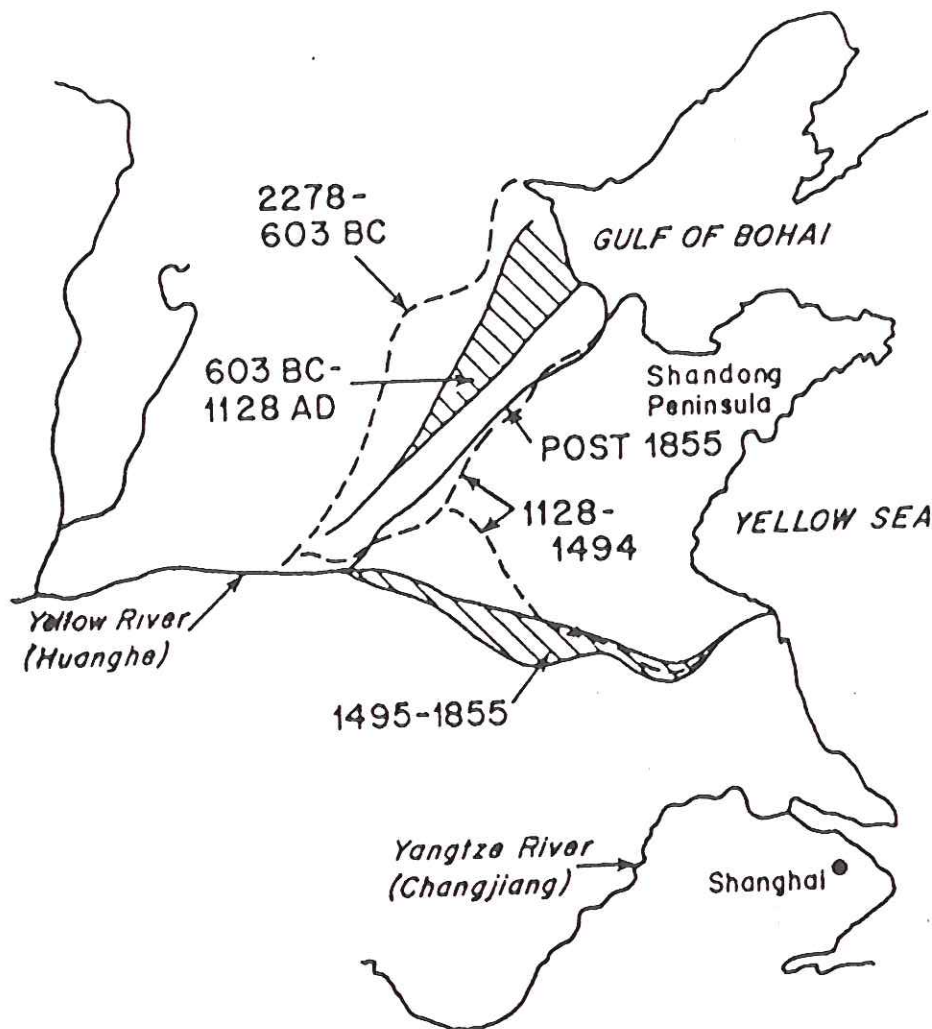
FIG. 2.—Paths of the Yellow River, 2278 BC to present. Years are in AD except where noted. Shaded areas refer to meandering river paths. Modified from Shen (1979).

TABLE 1

MAJOR EVENTS IN THE YELLOW RIVER DRAINAGE BASIN DURING THE PAST 2300 YEARS AND THEIR EFFECTS ON SEDIMENT DISCHARGE

Years	Event	Estimated %age of modern load	Estimated annual load ($\times 10^9$t)	Land over time interval ($\times 10^9$t)
600AD–present	Heavy agricultural usage; extensive erosion of loess plateau	100	1.2	1656
50AD–600AD	Mongol invasion; steppes return to grazing pastures	50	.6	324
200BC–60AD	Agricultural use, with many river channels diverting silt to the ocean	80	1.0	250
340BC–200BC	River channeled; loess plateau mostly forested; relatively little sediment lost by channel overflow	35	.4	59
			Total	2290

CHINA AROUND 1050 A.D.

⊙ Supreme Capital of Liao
○ Subordinate capitals of Liao

Amur River

Sungari R.

LIAO

HSI HSIA

Ta-t'ung

ORDOS

BORDER PREF.

Liao-yang

KORYŎ

Yen-ching (Peking)

Ning-hsia

Yellow River

Wei River

Kaifeng

Grand Canal

Huai River

SUNG

Chengtu

Yangtze River

Hangchow (Lin-an)

Tali

Ch'üan-chou

NAN-CHAO

Hsi (West) R. Canton

ANNAM
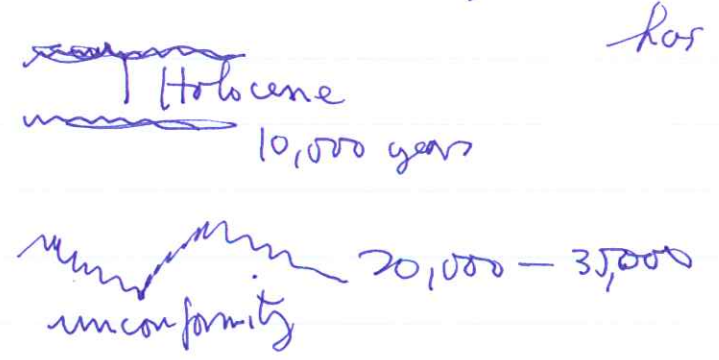
To find the pre-history value, they examined the sediment thickness on the bottom of the Yellow Sea, where all the sediment is ultimately deposited.

Fig. 1 shows ship tracks — conducted a seismic survey.

Fig. 3 shows a typical seismic section.

Erosional unconformity at 20K – 35K years — last ice age — Sea level lowered so China Sea was exposed.

^{14}C dating of cores shows that the dominant reflector labelled Holocene has an age of 10,000 years.

Holocene
10,000 years

20,000 – 35,000
unconformity

They measured the depth to this reflector over the entire basin — Fig. 4. — thereby added up the total volume of eroded sediment.
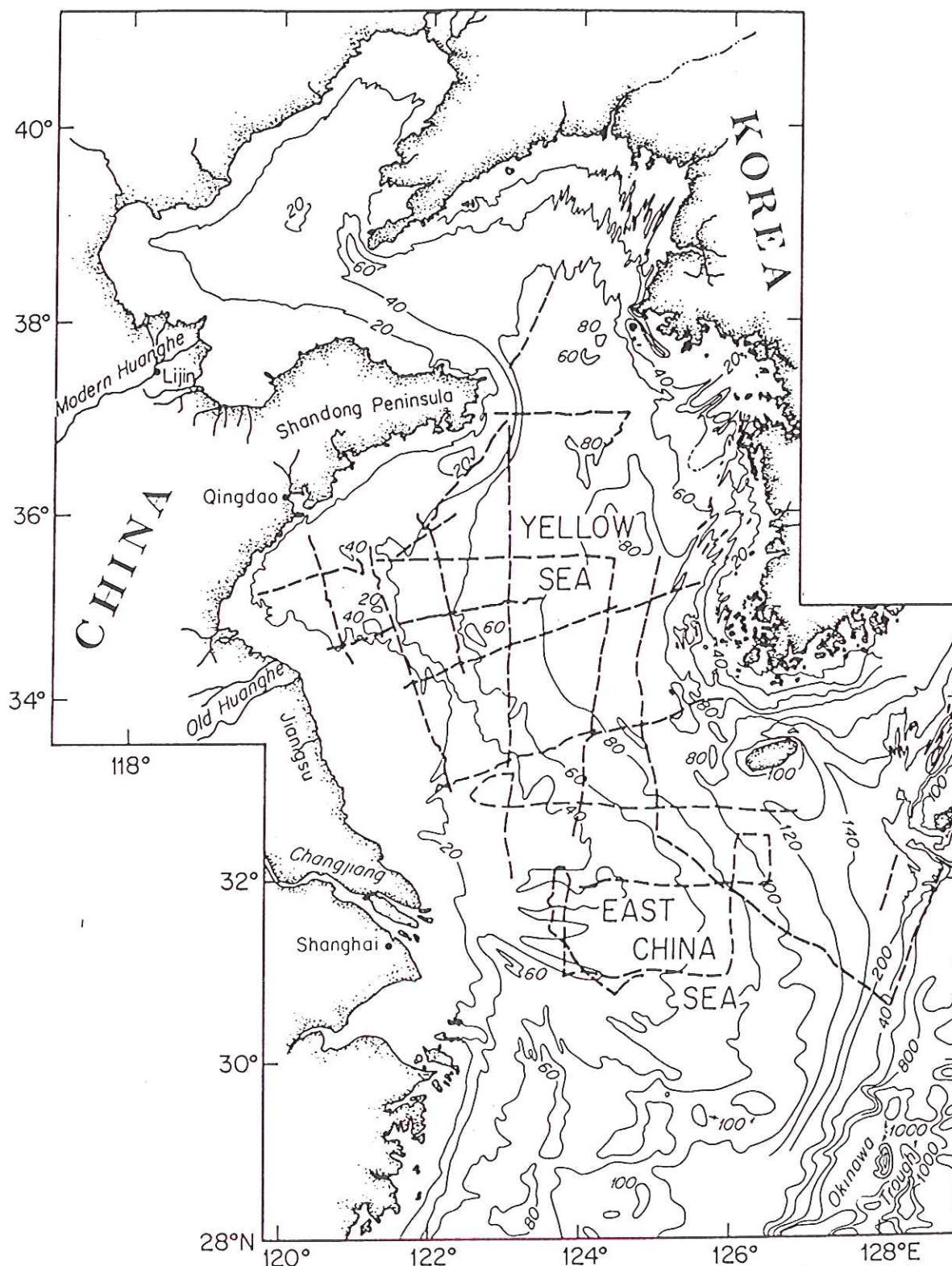
FIG. 1.—Bathymetric map of the Yellow Sea, showing location of seismic profiles taken between 1980 and 1986 which form the basis for the marine isopachs shown in figure 4. Arrows off Jiangsu coast show location of profile shown in figure 5. Depths in meters.
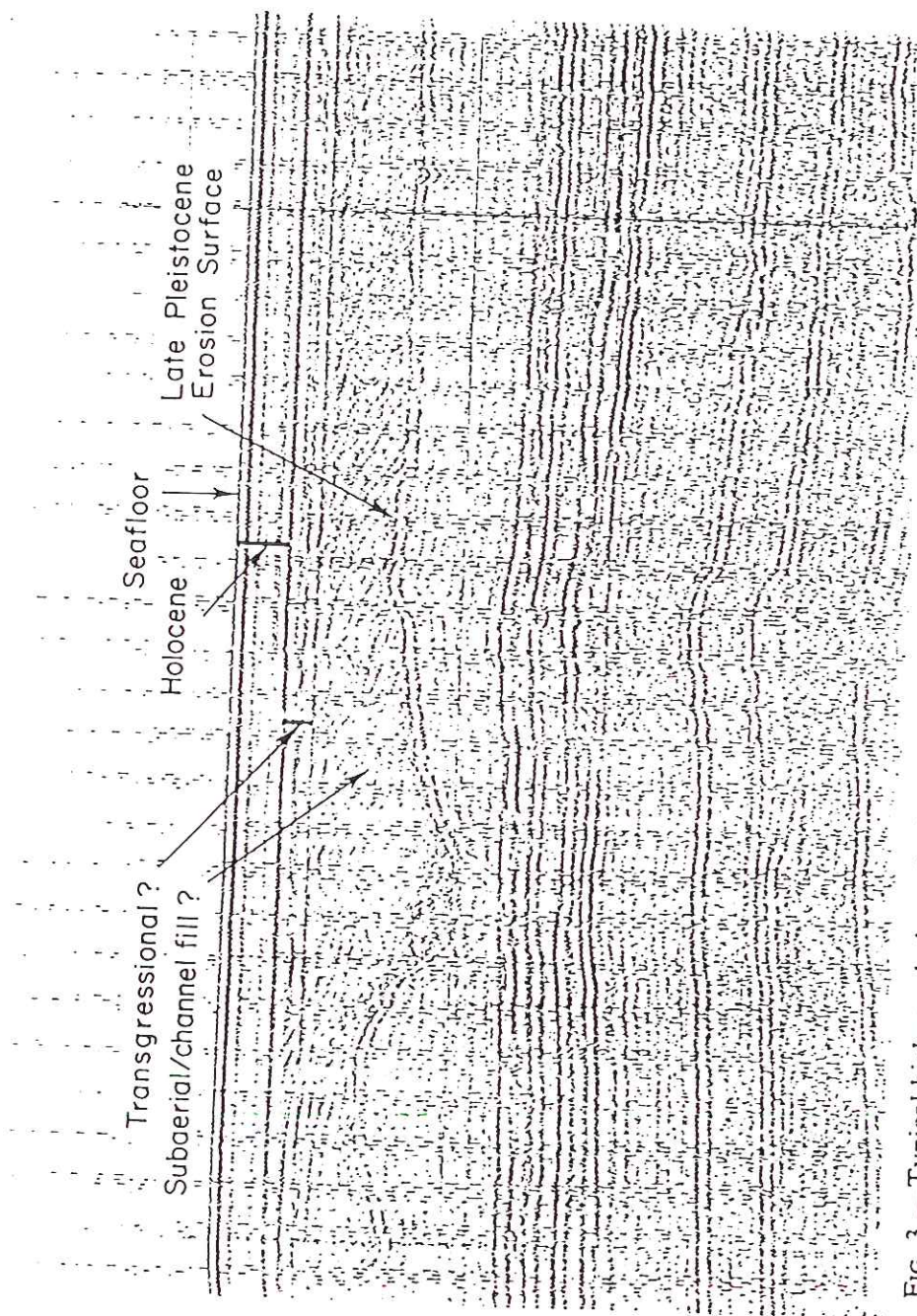
FIG. 3.—Typical high-resolution seismic profile from the central Yellow Sea, southeast of the Shandong Peninsula showing late Pleistocene erosion surface (and possible channel), infilled sediment (channel sands?), a transgressional layer (presumably sand and peat), and an acoustically transparent surface sequence (Holocene neretic muds). Length of record is 40 minutes, or about 4.5 km. Distance between vertical (scale) lines is 25 ms.
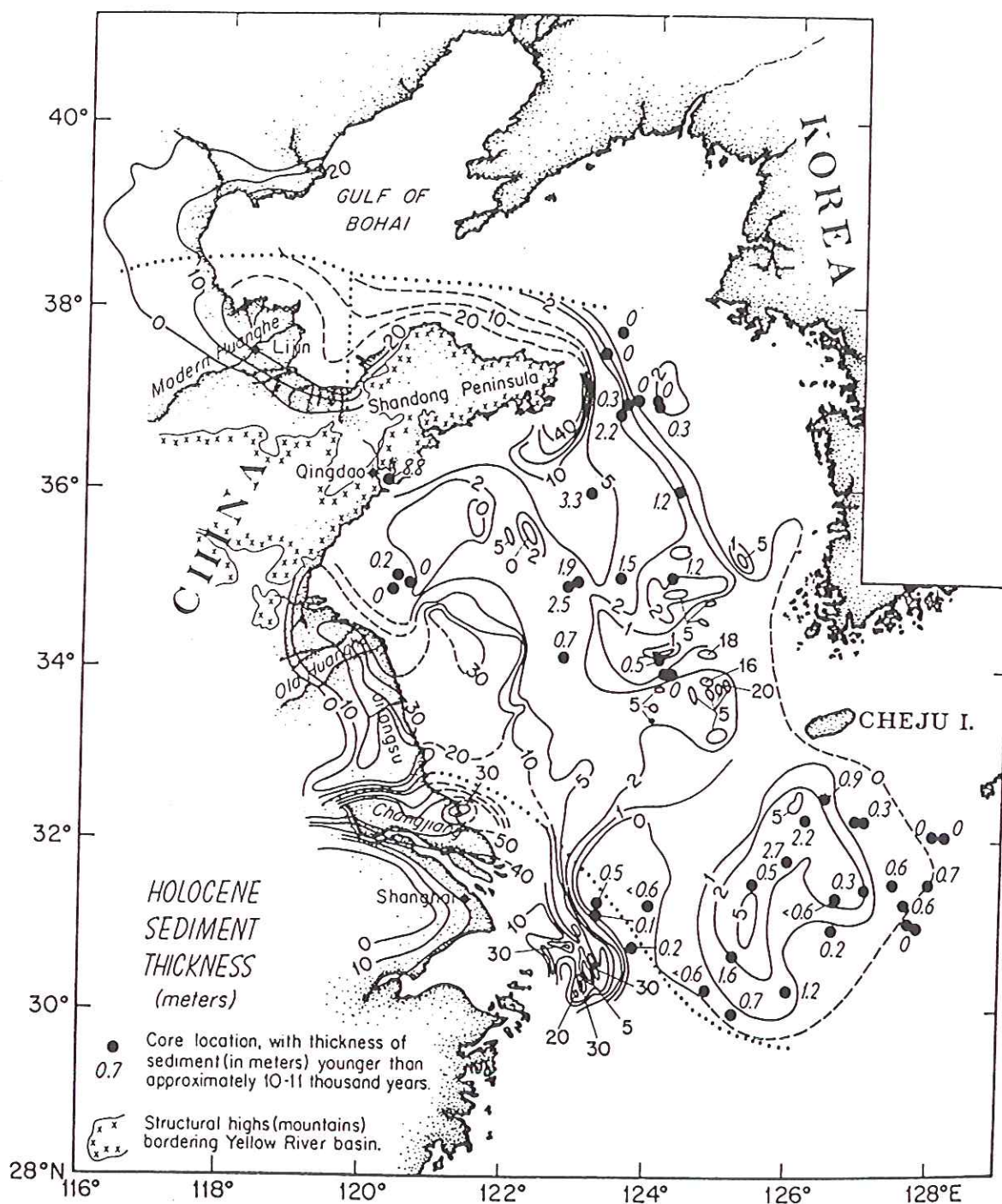
FIG. 4.—Thicknesses of Holocene marine sediment interpreted from land-based and marine-seismic data. Thicknesses are in meters. Sediment isopachs off the Yangtze River are from Gao et al. (1982). Dots with numbers designate Holocene sediment thicknesses (in meters) penetrated by cores; data from Yanagida and Kaizuka (1982), Wang and Wang (1982), Liu et al. (1983), Peng et al. (1984), and Chen et al. (1985). Dotted lines show the approximate north and south boundaries of Yellow-River sediment. Sediment volumes were computed within these boundaries. The N-S dotted line east of Lijin represents the assumed boundary between the northern delta and the Shandong mud wedge; in reality these two features are continuous, and the mud wedge in fact at least partly may represent an older delta.

Table 2 shows their final result —
they to correct for escaping sediment
out of the study area (a 6% effect)

Conclusion:

farming era

$$\frac{2300 \cdot 10^9 \text{ tons sediment}}{2300 \text{ years}} \approx 10^9 \text{ tons/yr average}$$

non-farming era

$$\frac{(3000 - 2300) \cdot 10^9 \text{ tons}}{10,000 - 2300 \text{ years}} \approx 10^8 \text{ tons/year average}$$

Man's cultivational practices over the
past ~2000 years in the easily eroded
loess of China has increased the
erosion rate by a factor of 10!

A huge effect ⟹ need to be careful
about modern-day stream-load ~~measurements~~
measurements.

Berner analysis (homework problem) shows that
the effect of man in US has been more
like a factor of 2-3

TABLE 1

Major Events in the Yellow River Drainage Basin during the Past 2300 Years and Their Effects on Sediment Discharge

Years	Event	Estimated %age of modern load	Estimated annual load ($\times 10^9$t)	Land over time interval ($\times 10^9$t)
600AD–present	Heavy agricultural usage; extensive erosion of loess plateau	100	1.2	1656
50AD–600AD	Mongol invasion; steppes return to grazing pastures	50	.6	324
200BC–60AD	Agricultural use, with many river channels diverting silt to the ocean	80	1.0	250
340BC–200BC	River channeled; loess plateau mostly forested; relatively little sediment lost by channel overflow	35	.4	59
			Total	2290

TABLE 2

Volume of Sediment in Various Areas and Facies

	Volume (km³)	% of Total Holocene Shelf Sediment
Distal Mud Lens	360	13
Cheju Mud Patch	110	4
South Delta	1290	46
North Delta	540	19
Shandong Mud Wedge	510	18
SUBTOTALS	2810	100
Escaping Shelf	200	
TOTAL SEDIMENT		3000

Note.—The distal mud lens is defined as those sediments between 0 and 5 m in thickness, excluding the Cheju mud patch. The Cheju mud patch refers to the local thickening of sediments thicker than 5 m. The Shandong mud wedge is presumed to be the distal portion of the north delta; it is defined as those sediments north and south of the Shandong Peninsula and east of approximately 120°E that are thicker than 5 m (see fig. 4).

Erosion rates of major river basins of world

chemical erosion rate in Tg/million sq km

total erosion rate Tg/million sq km

Irrawaddy

Bramaputra

Ganges

Huanghe

Yangtze

correction for influence of man's agricultural practices
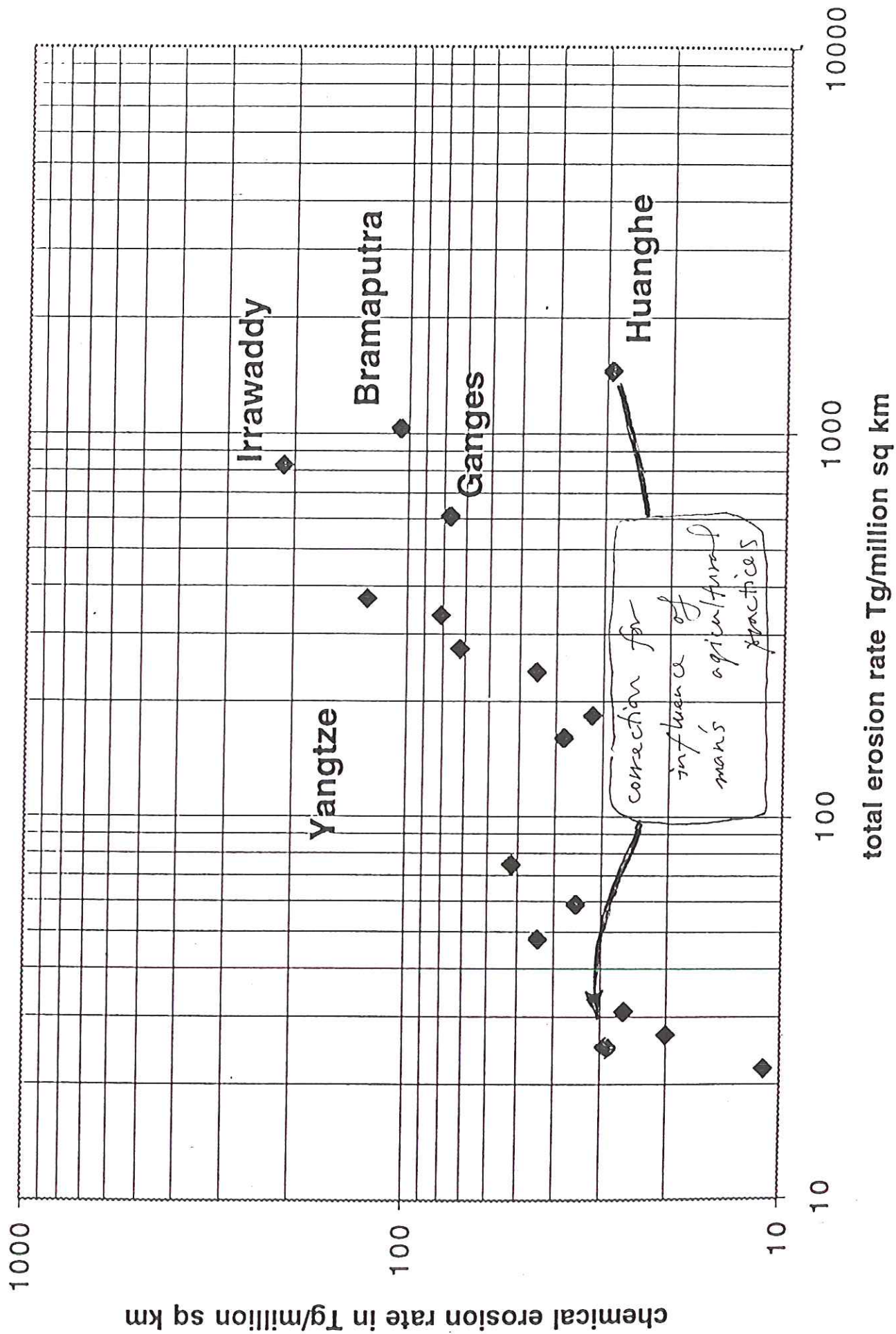
$$\epsilon = -\lambda h. \tag{2}$$

Thus, the observed linear relationship between relief h and erosion rate ϵ is consistent with the idea of an inexorable decay of the landscape, at least in these mid-latitude drainage basins.

However if, as pre-Huttonian Christian geologists, we begin to push our inquiry somewhat further, we start to run into problems with our world view. For example, with our quantitative erosion data (Fig. 1) and the decay equation (1) we can calculate a *topographic half-life*, $t_{1/2}$, for decay of an initial topographic relief h_o to half its value:[10]

$$t_{1/2} = \ln \frac{2}{\lambda}, \tag{3}$$

The topographic half-life for the mid-latitude basins (Fig. 1) from this analysis is about 5 million years, so from a quantitative point of view the decay of the Earth would only have just begun for the pre-Huttonian geologist. Similarly the time required to go backward to a topographic relief that is twice the present value also requires 5 million years, which is quite long relative to the pre-Huttonian view of a young Earth.

Thus, as pre-Huttonian Christian geologists living in large mid-latitude drainage basins we would begin to either question some point of our analysis or to question our belief of a young, inexorably decaying Earth. We would probably check our analysis in various ways, for example by making minimum estimates of the volume of material removed from valleys that are cut into originally continuous layers of rock, then dividing the volume by the measured erosion rate. The answer we would get from this estimate is again in the millions of years. Once again we would be pressed to consider that it took a long time to make the mid-latitude landscape of Britain and the eastern United States. There are many other tests we could apply—for example considering substantial temporal variation in erosion rates—but eventually the weight of evidence would impel us to abandon our belief in a young, inexorably decaying Earth. In fact today there are few pre-Huttonian Christian geologists, even though there are many Christian geologists.

The Inexorable Erosion of Taiwan

I am now going to inflict you with an account of erosion on an island in East Asia. The reason for doing this is to show in microcosm where the Huttonian assumption of uniformitarianism has got us in knowledge of the Earth in 200 years. It will serve as an example of scientific knowledge claims, which will come in handy later on when we consider Christian knowledge claims.

Now erosion rates are not generally such a simple function of relief as we considered above (eq. 2), particularly in mountainous regions where rates are dominated by chemical processes and climate, which cause the rates to vary over many orders of magnitude. Some of the highest erosion rates in the world have been measured on the very mountainous Island of Taiwan.[11] In the following paragraphs we estimate the rate of erosion of Taiwan in five or six ways that are either wholly or partially independent and get essentially the same answer, about 5-6 mm/y or 5-6 km per million years (km/my), measured over timescales of 50 years to 2 my. We find that this numerical agreement—of only minor importance in itself—serves as an epistemic glue that links into a rather strong web of knowledge claims, the diverse ideas and measurements that contributed to the estimates.

---

[10]that is, by setting $h_o = 2h$ in equation 1

[11]Milliman and Meade 1983

widths of about 90 km that persists over most of the Island of Taiwan. According to the time-space equivalence, the constant width predicts that the mountains are topographically in steady state; that is, the compressive flux of 500 km^2 must be balanced by an equivalent erosive flux. Given the width of mountains of 90 km, we would calculate an erosion rate of about 5-6 mm/y (5-6 km/my), which agrees with our previous estimates. This however requires that Taiwan is indeed a topographically steady-state mountain belt, that the time-space equivalence is correct, and that the quantitative solution for present-day plate tectonics is also essentially correct. The rates of plate tectonics ultimately depend on radioactive decay of K^{40}, slip vectors on plate boundaries determined from earthquakes, the orientations of transform faults and the modelling of marine magnetic anomalies in the Atlantic, Indian, and Pacific Oceans, all of which are independent of erosion rates measured from stream-load data and are independent of the estimates from cooling of rock, except for the decay constant of K^{40}.

Erosion rates from uplifted reefs and steady-state topography. If the the mountain belt of Taiwan is topographically steady-state, as suggested by the analysis above, then on the average mountains are uplifting as fast as they are eroding. Thus data on uplift rate should be equal to data on erosion rate. In southern and eastern Taiwan there are uplifted Holocene reefs and marine terraces that contain fossil corals dated by C^{14}, yielding uplift rates of about 5 km/my over the last 5000 to 10,000 years, in good agreement with the erosion rates and the concept of steady-state topography.[16] The measurement of uplift of the reefs is independent of all the erosion estimates.

Erosion rates from sediments deposited offshore of Taiwan. Essentially all detritus eroded from the mountains of Taiwan is washed into the sea and deposited in adjacent sedimentary basins: in the Philippine Sea, South China Sea, Okinawa Trough, and Taiwan Strait. By measuring the thickness of sediment in these basins off Taiwan we could also estimate an erosion rate. This has not been done; it is actually a rather complex task because of the need to determine the horizontal extent of layers of any given age near Taiwan. However it is known that the sedimentation rates near Taiwan are among the highest in the world (1-10 km/my over the last 0.5-3 m.y.) and are thus in at least semiquantitative agreement with the erosion rates.[17] The sediments are dated largely by marine nannofossils whose absolute ages are ultimately based on the magnetic reversal timescale calibrated by radiometric dates involving K^{40} decay. This is the same timescale used in the computation of plate motions, mentioned above.

History of erosion from sediments deposited offshore of Taiwan. The sedimentary basins around Taiwan are important to us beyond their record of sedimentation rate. The details of the sedimentary record—bed-by-bed—provides an elaborate, detailed record of the history of erosion. Each bed, usually about 1 cm to 1 m thick, provides a record of a depositional event, in many cases storms.[18] Furthermore, studies of changes in the composition of rock fragments eroded from Taiwan over entire stratigraphic sequences representing several million years, records a progressive unroofing

---

[16] Peng and others, 1977.

[17] Chi and others, 1981; Chi and Chang, 1983.

[18] Covey 1984, 1986; Dorsey and Lundberg 1988. Thus we might we might say that a particular 70 cm thick layer of sediment records the the great typhoon of October 897,246 B.C. We can't assign calendar years with great certainty but we might tell the month by the growth lines on all the clam shells included in the bed. The point is, we are dealing with specific, detailed history, not just the numerical value of an erosion rate.

of deeper and deeper metamorphic rocks in the mountains of Taiwan, from which erosion rates on the order of 4-6 km/my are estimated based on the ages of the sediments and the estimated depths of metamorphism recorded in the rock fragments.[19]

Erosion and Epistemology

By now you should have asked, "What did I do to deserve being inflicted with an account of the erosion of some island in the Far East?" Have we learned anything about the epistemology of science and Christianity from this excursion into the erosion of Taiwan?

First, we have learned that uniformitarianism is correct in this case and Hutton would have been happy. Present-day erosion rates averaged over the last 50-100 years are indeed in complete agreement with those measured independently by a varienty of methods over time scales ranging from 5-10,000 years to 1-2 million years. Secondly, we have learned that the mountains of Taiwan are not inexorably decaying away as the pre-Huttonians would have thought. They are topographically steady-state, that is, the mountain growth and the erosion are in balance. The pre-Huttonian world-view is wrong for the Island of Taiwan. Thirdly, we have learned that we can gain confidence in a whole system of truth claims by a set of wholly and partially independent checks. We gained confidence not just in our numerical erosion rates, which is of minor significance, but, much more importantly, in all the wholly or partially independent observations and ideas that contributed to the estimates. The web of observations and ideas, as diverse as stream gauge measurements, plate tectonics, widths of the mountain ranges, and cooling of minerals, is linked together by the numerical agreement of the erosion rates.

If, as a Christian geologist, I were to still insist on the pre-Huttonian world view of a young and decaying Earth in the face of observations such as these, I would be forced to follow a path of grave theological danger in which I would be claiming that the intricate system of wholly and partially independent checks of knowledge claims that are routine in geology are an effect of a Universe that is a façade. For me to hold the pre-Huttonian world view, having participated in much of the work in Taiwan, would be Christian heresy. That's why I'm not pre-Huttonian.

Where the Pre-Huttonian Christian Geologists Went Wrong

The true pre-Huttonian Christian geologists of the fifteenth to eighteenth centuries—not our rhetorical ones—were not heretics, they were just mistaken about a number of things. Perhaps we can learn from their mistakes:

Age of the Earth. Perhaps the most obvious mistake of the pre-Huttonians is that they didn't recognize the order of magnitude of geologic time. Had they actually measured stream loads and compared them with either volumes of valleys or thicknesses of sequences of strata they would have been aware of ages of at least millions of years.[20] The order of magnitude of geologic time was not known with much certainty to most geologists until soon after the first radiometric dates were obtained by Boltwood and others in the first decade of this century, which indicated ages on the

---

[19] Lee 1977; Dorsey 1988

[20] Some were aware of evidence for ages beyond the Ussherian timescale, *see* Davies.

Climate-Driven Bedrock Incision in an Active Mountain Belt

Karen Hartshorn,[1] Niels Hovius,[1] W. Brian Dade,[2]
Rudy L. Slingerland[3]

Measurements of fluvial bedrock incision were made with submillimeter precision in the East Central Range of Taiwan, where long-term exhumation rates and precipitation-driven river discharge are independently known. They indicate that valley lowering is driven by relatively frequent flows of moderate intensity, abrasion by suspended sediment is an important fluvial wear process, and channel bed geometry and the presence of widely spaced planes of weakness in the rock mass influence erosion rate and style.

The links between the tectonic uplift, climate, and denudation of an active mountain belt are forged in bedrock river channels (1, 2). Fluvial incision of uplifted bedrock lowers the base level and drives mass wasting of adjacent hillslopes. The resulting debris is eventually deposited onto valley floors, where it enhances or impedes fluvial wear of the channel bed (1–3). Where fluvial wear does not check rock uplift, the region's relief, steepness, and orographic precipitation rates rise until steepened river slopes and enhanced discharge allow fluvial erosion to balance tectonic uplift once again.

The mechanics of fluvial wear are commonly considered in terms of average flow conditions and abrasion due to bedload transport (1, 4, 5), but few observations are available to validate these assumptions (6–8). The role of average versus extreme flows in producing erosion is unknown, as is the relative importance of abrasion and wear by particles in turbulent suspension. Here we present observations of fluvial bedrock incision due to moderate and extreme discharges from the LiWu River in the eastern Central Mountain Range of Taiwan (Fig. 1) to help address these questions. Originating at 3500 m above sea level, the LiWu River drains approximately 600 km² of steep terrain underlain by metasedimentary rocks. The area has high rates of tectonic uplift [3 to 6 km per million years (My^{-1})] and sediment yield, indicating strong forcing and the presence of natural tools for incision by abrasion (9–12). Approximately 10^7 metric tons of sediment move through the river each year, or about 0.1% of the global supply of sediment to the sea (13).

Daily hydrological records for the LiWu River span 40 years (14). Discharge during typhoons can exceed the long-term daily average by an order of magnitude or more. In

August 2000, Supertyphoon Bilis produced a flood in the LiWu River (Fig. 2, A and B) peaking at 2240 m³ s⁻¹, or about 65 times the daily average discharge of 36 m³ s⁻¹ from 1960 to 2001. Such floods have dramatically elevated sediment loads (3) (Fig. 2C). No sediment data are available for Supertyphoon Bilis, but from other available records for 1982 we estimate that approximately 90% of the total sediment discharge, and 15% of the total water discharge of that year, occurred over 5 days during a similar typhoon-driven flood (14). No major storms crossed the LiWu catchment during the dry season after

August 2000 or in the following wet season of 2001 (Fig. 2A).

To document the ongoing incision of the LiWu River, we established a field site with representative channel geometry near the only gauging station in the catchment (Fig. 1). The upstream drainage area is 435 km², and the channel slope averaged over a 1-km reach spanning the site is 0.02. The continuously exposed bedrock at the site comprises schists and a prominent quartzite bed that runs across the channel (Fig. 1). These two lithologies dominate the upper catchment and have contrasting properties. The schists are densely foliated, and a conventional field measure (22 on a Schmidt hammer scale) (15) indicates low compressive strength; a single tensile strength test, using the Brazilian tension splitting method, yielded a value of 5.3 MPa. The quartzite is massive, with relatively continuous joints spaced at decimeter intervals, and exhibits intermediate compressive strength (Schmidt hammer scale 63) and a tensile strength of 9.5 MPa. The tensile strengths of both rock types are within the normal range for metasedimentary rocks (8). In an abrasion mill test, the schist was found to abrade approximately four times faster than the quartzite (8, 16, 17).

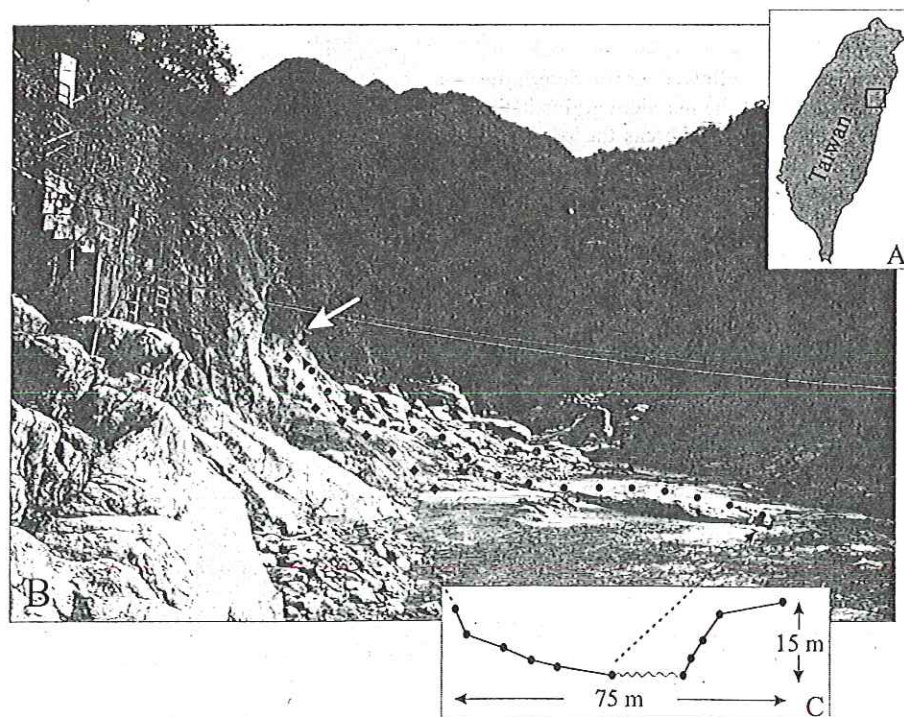Our site covers most of the active channel of the LiWu River, which has a parabolic cross

Fig. 1. (A) Location of study site within Taiwan. (B) Photograph of site from upstream. Black circles represent the location of transect drilled and measured on quartzite, and black diamonds represent the location of the schist transect. White arrow shows the high-water mark, approximately equivalent to the high point of Supertyphoon Bilis. The metal cage and overhead cables indicate the location of discharge and the suspended sediment gauging station. (C) Cross section of the channel along the quartzite outcrop with survey points, showing characteristic parabolic shape with steep side walls. The wavy line represents the low-water mark.

[1]Department of Earth Sciences, [2]Institute of Theoretical Geophysics, University of Cambridge, Downing Street, Cambridge, CB2 3EQ, UK. [3]Department of Geosciences, Pennsylvania State University, 503 Deike Building, College Park, PA 16802–2714, USA.

section and a locally well-developed inner channel (Fig. 1C). The active channel is defined overall as the wetted perimeter of the maximal flood and is delimited by the lower margin of dense forest cover of adjacent hillslopes. From February 2000 to December 2001, we conducted four detailed surveys of channel bedrock elevation at 20-mm intervals, using an array of permanent, recessed, and evenly spaced benchmarks (Fig. 1B). Vertical erosion at a point is estimated as the change in bedrock topography incurred during an interval between surveys, with the understanding that most of the measured signal may be associated with one or a small number of exceptional discharge events. Standard errors of repeat measurements of bedrock topography along a reference transect well above the high-water mark indicate a precision of 0.5 mm or better. This level of precision did not vary within or between field seasons. We focus here on results from two survey transects oriented perpendicular to the channel to sample erosion at representative elevations between

characteristic low- and high-water levels. One transect is 24 m in length in schist, and the other is 42 m long in quartzite. Together, these transects comprise 2109 measured points.

Our surveys captured changes during an active typhoon season (the wet season of 2000), a dry season (the dry season of 2001), and a relatively inactive typhoon season (the wet season of 2001) (Fig. 2A). Median estimates of erosion across the active channel and for the entire period from February 2000 to December 2001 were 8.5 mm for the quartzite and 6 mm for the schist. However, important spatial and temporal patterns emerged during the course of our study, with maximal local erosion of 182 mm in quartzite and 69 mm in schist.

Erosion in both lithologies was greater, by up to an order of magnitude, during the wet season of 2000 than during the subsequent dry and wet seasons of 2001 combined (Fig. 3). Maximal values of spatially averaged erosion were 82 mm in the quartzite and 36 mm in the schist for the period between February and December 2000. In contrast, analogous values of erosion were 6 and 2 mm, respectively, for the period from December 2000 to December 2001.

Erosion peaked at higher elevations within the active channel during the 2000 wet season than during the dry and wet seasons of 2001. In particular, wear was greatest between 2 m and 6 m above mean low-flow level in the quartzite and between 3 m and 7 m above mean low-flow level in the schist. Above these elevations, spatially averaged wear of several millimeters occurred up to the flood line of Supertyphoon Bilis, at about 10 m above the mean low-flow level. Low in the channel, the erosion rate dropped significantly. In contrast, erosion during the 2001 dry and wet seasons mostly occurred less than 3 m above mean low-flow level, with wear rates increasing toward the low-flow line (Fig. 3).

High erosion rates in quartzite reflect to some degree its current relatively exposed aspect elevated above the schist (Fig. 1) and the effect of controls on erosion resistance, such as

spacing and condition of joints, that are not captured by usual measures of rock strength (8). Rock mass properties contribute as controls on the style of erosion, with a greater spread and more irregular distribution of erosion in the broadly jointed quartzite than in the densely foliated schist (Fig. 3). As an example, a coefficient of variation for the spatial interval exhibiting maximal average erosion, and defined as the ratio of the range of observations in the central quartiles to the median of observations, is 1.04 for the quartzite during the 2000 wet season and 4 during 2001. The analogous values for schist were 0.58 and 1.0, respectively. The different values reflect an order of magnitude decrease of median wear rates between the wet season of 2000 and the wet and dry seasons of 2001, paired with only a twofold reduction of the range of wear rates in the central quartiles. We propose that the differences in the relative spread of wear rates are associated with the removal of joint-bound blocks, which are decimeters in size, from the quartzite. The removal of quartzite blocks is visible through before-and-after measurements of the topography (fig. S1) and was prominent at intermediate elevations in the channel where erosion rates were largest. In February 2000, these blocks were firmly lodged in the channel bed in locations with relatively little lateral support, and we suspect that fracturing was needed for their removal, in addition to hydraulic forces (18). Similar removal of blocks was not observed in the adjacent schists (fig. S1). Observed lithological and spatial differences in wear are consistent with the notion that, where and when active, the removal of blocks is a more effective style of fluvial bedrock erosion than abrasion (2, 4, 18).

In addition to block removal, we consider small-scale abrasion to be the likely cause of much erosion at intermediate flow levels during floods. Peak flow conditions during Supertyphoon Bilis (flow depth $h = 12$ m, channel slope $s = 0.02$) correspond to bed shear stress in excess of 2000 Pa, which is sufficient to move boulders with diameter d of up to 3 m as bedload. The average eleva-
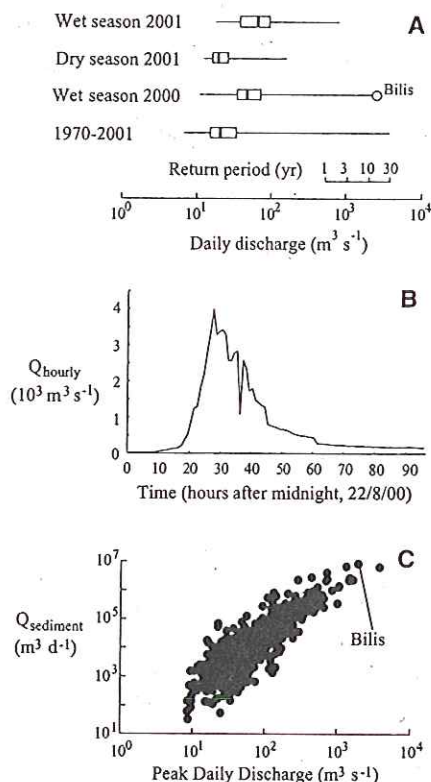
Fig. 2. (A) Box plot summarizing LiWu hydrology during indicated periods. The heavy vertical lines indicate median values, boxes enclose the central two quartiles, and whiskers indicate the full range of daily discharge values. The peak day-long discharge associated with Supertyphoon Bilis, in August 2000, is indicated by the open circle. Return period of exceptional floods shown for reference. **(B)** Hourly hydrograph of discharge (Q) at the field site associated with Supertyphoon Bilis, for 96 hours after midnight, 22 August 2000. **(C)** Sediment rating curve for all events observed in LiWu catchment from 1970 to 2001. Discharge and the predicted sediment discharge point for Supertyphoon Bilis are indicated.

Fig. 3. Erosion rates for schist **(A)** and quartzite **(B)** through the typhoon 2000, dry 2001, and typhoon 2001 seasons. Boxes represent median values of erosion rates as a function of elevation above the low-flow line, and whiskers represent 25th- and 75th-percentile values. Elevation range has been divided into 50-cm intervals, and all measurements within an interval combine to produce the median values for that elevation. Open boxes represent the combined median values from the wet season of 2000, and inset black boxes represent combined median values from subsequent seasons, including the dry season and inactive wet season of 2001. Inset graphs have same axis labels as the larger graphs. Erosion rates represent vertical (downward) erosion at a point, not widening or horizontal values.
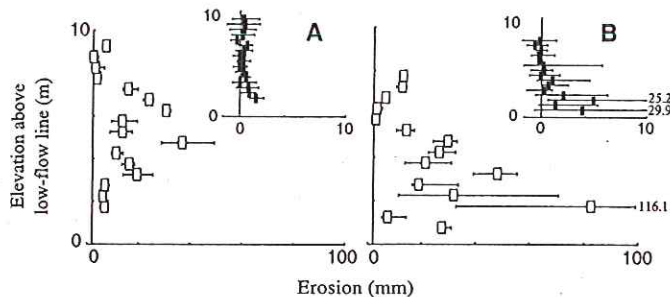
tion achieved by bedload particles can be given in terms of fractional depth Z_b and relative grain size $D = d/h$ by

$$Z_b = AD\theta^{1/2} \qquad (1)$$

where $\theta = sh/Rd$ with $R = 1.65$ for quartz grains in water and the empirical dimensionless coefficient $A \approx 4$ for irregularly shaped particles (19). Thus, a meter-sized boulder would have bounced up to several meters above the bed during peak flood conditions. Sediment of this caliber is relatively rare in the LiWu channel, because the schists that dominate the upper catchment produce much finer debris. In extreme floods, such material would travel in turbulent suspension.

In a channel that is steep-walled and parabolic in cross section, the vertical distribution of particles suspended in simple channel flow can be described generally with a single expression (20). Mathematical averaging of this expression over the relative depth range $\{Z_b, 1\}$ yields the fractional depth Z_s, above which the concentration of suspended particles of a given size decays significantly from its near-bed maximum nominally taken at Z_b. Thus, Z_s is given by

$$Z_s = \frac{Z_b^P - Z_b}{(1 - P)(1 - Z)} \qquad (2)$$

where $P = 2.5\,\theta^{-1/2}$ for medium sand and larger particles. From Eqs. 1 and 2, we find that only particles for which $P < 0.3$ (or $\theta > 70$) would have traveled in significant numbers at elevations greater than $0.3\,h$ or, equivalently, at >4 m above the bed during peak flood. Such particles have diameters of about 2 mm or less. Thus, we propose that maximal wear rates at midlevels of peak flow are due to rare but significant impacts of large boulders saltating along the bed and to more or less continuous abrasion by very coarse sand and finer material in suspension transport.

Spatially averaged erosion of both rock types between December 2000 and December 2001 approached values of 2 to 6 mm year^{-1} and occurred near the base of the channel. These incision rates are in good agreement with independent estimates of long-term exhumation at 3 to 6 mm year^{-1} mentioned above. During the 2000 wet season, in contrast, spatially averaged wear of both rock types locally exceeded 10 mm to a significant degree, with maximal values observed at greater elevations on the channel wall. This work is assumed to be predominantly a result of Supertyphoon Bilis, because other floods failed to reach that high in the channel. The return period for events equal to or greater than Supertyphoon Bilis is estimated to be about 20 years (Fig. 2A) (14). Prorated for this frequency, the maximal spatially averaged erosion rates for the 2000 wet season were 5.5 mm year^{-1} for quartzite and 2.3 mm

year^{-1} for schist, but corresponding values for the base of the channel were only 1.7 mm year^{-1} for quartzite and 0.3 mm year^{-1} for schist. This suggests that erosion rates associated with exceptional events fail to balance estimates of long-term exhumation rates throughout the active channel. Our data indicate that the lowering of the LiWu valley is driven by relatively frequent flows of low to moderate intensity (21) and that rare large floods are more important in widening the bedrock channel than they are in driving down the base level. However, such floods help transmit the effect of accumulated thalweg lowering to adjacent hillslopes.

References and Notes
1. A. D. Howard, W. E. Dietrich, M. A. Seidl, *J. Geophys. Res.* **99**, 13971 (1994).
2. G. S. Hancock, R. S. Anderson, K. X. Whipple, *Geophys. Monogr.* **107**, 35 (1998).
3. N. Hovius, C. P. Stark, H. T. Chu, J. C. Lin, *J. Geol.* **108**, 73 (2000).
4. K. X. Whipple, N. P. Snyder, K. Dollenmayer, *Geology* **28**, 835 (2000).
5. D. P. Finlayson, D. R. Montgomery, B. Hallet, *Geology* **30**, 219 (2002).
6. K. Tinkler, E. E. Wohl, *Geophys. Monogr.* **107**, 1 (1998).
7. J. Lave, J. P. Avouac, *J. Geophys. Res.* **106**, 26561 (2001).
8. L. S. Sklar, W. E. Dietrich, *Geology* **29**, 1087 (2001).
9. L. S. Teng, *Tectonophysics* **183**, 57 (1990).
10. T. K. Liu, S. Hsieh, Y. G. Chen, W. S. Chen, *Earth Planet. Sci. Lett.* **186**, 45 (2001).
11. M. G. Bonilla, *Geol. Soc. China Mem.* **2**, 43 (1977).
12. P. M. Liew, M. L Hsieh, C. K. Lai, *Tectonophysics* **183**, 121 (1990).
13. J. D. Milliman, J. P. M. Syvitski, *J. Geol.* **100**, 525 (1992).
14. *Hydrological Yearbook of Taiwan, R.O.C.* (Water Resources Bureau, Taipei, Taiwan, 1960–2000).
15. M. J. Selby, *Zeitschr. Geom.* **24**, 31 (1980).
16. L. Sklar, personal communication.
17. The abrasion mill was loaded with 150 g of 6-mm gravel and was run at 1000 rpm.
18. K. X. Whipple, G. S. Hancock, R. S. Anderson, *Geol. Soc. Am. Bull.* **112**, 490 (2000).
19. W. B. Dade, A. R. M. Nowell, *Euromech* **310**, 201 (1994).
20. G. V. Middleton, J. B. Southard, *Mechanics of Sediment Movement* (Society of Economic Paleontologists and Mineralogists, Tulsa, OK, 1984).
21. M. G. Wolman, J. P. Miller, *J. Geol.* **68**, 54 (1960).
22. This study was funded by NSF grant EAR-9903196 to R.L.S. and N.H. K.H. and W.B.D. are supported by the U.K. Natural Environmental Research Council. Thanks to L. Sklar for measuring tensile strength and erodibility of lithologies at our study site and giving feedback on the manuscript; to two anonymous reviewers for their insight and improvements; to M. Chen, S. Dadson, and D. Kitching for invaluable help in the field; and to the Taroko National Park authorities for generous logistic support.

Uplift in the Fiordland Region, New Zealand: Implications for Incipient Subduction

M. A. House,[1]* M. Gurnis,[1] P. J. J. Kamp,[2] R. Sutherland[3]

Low-temperature thermochronometry reveals regional Late Cenozoic denudation in Fiordland, New Zealand, consistent with geodynamic models showing uplift of the overriding plate during incipient subduction. The data show a northward progression of exhumation in response to northward migration of the initiation of subduction. The locus of most recent uplift coincides with a large positive Bouguer gravity anomaly within Fiordland. Thermochronometrically deduced crustal thinning, anomalous gravity, and estimates of surface uplift are all consistent with ~2 kilometers of dynamic support. This amount of dynamic support is in accord with geodynamic predictions, suggesting that we have dated the initiation of subduction adjacent to Fiordland.

The response of plate boundaries to the initiation of subduction remains a fundamental, unsolved problem in plate tectonics (1). Geodynamic models of subduction initiation generally predict the plate over a newly descending slab will be dynamically uplifted during

the first few million years after the initiation of convergence (1, 2). The rate of uplift will be proportional to the rate of convergence whereas the amount of uplift will be proportional to the amount of total compression, at least during the early phase of subduction nucleation (1). As a consequence of this dynamic support or uplift, a strong positive gravity anomaly would develop on the overriding plate as the base of the crust is progressively uplifted over time.

The apparently young plate boundary adjacent to the Fiordland region of South Island, New Zealand, along with its offshore

[1]Division of Geological and Planetary Sciences, Caltech, Pasadena, CA 91125, USA. [2]Department of Earth Sciences, University of Waikato, Hamilton 2001, New Zealand. [3]IGNS Ltd., Lower Hutt, Private Bag 30368, New Zealand

*To whom correspondence should be addressed. E-mail: mhouse@gps.caltech.edu